A COMPUTER SIMULATION STUDY OF DISLOCATION MOTION IN THE MODIFIED FRENKEL-KONTOROVA MODEL

by

Bülent Tepebağ

Submitted to the Faculty of Engineering
in Partial Fulfillment of
the Requirements for the Degree of
MASTER OF SCIENCE
in
MECHANICAL ENGINEERING

Boğaziçi University
1982

THIS THESIS HAS BEEN APPROVED BY :

Dr. Sabri Altıntaş
(Thesis Supervisor)

S. Altıntaş

Doç.Dr. Öktem Vardar

Öktem Vardar

Doç.Dr. Başar Civelek

M. Başar Civelek

ABSTRACT

In this thesis, the motion and vibration characteristics of edge dislocations are investigated. Topics included, are shear stress-dislocation velocity relation; effects of model parameters and phenomenological damping on the dislocation motion; motion of a dislocation in a lattice with some impurities such as one or two fixed atoms; vibration characteristics of pinned dislocations; effects of temperature, damping and geometric parameters on the vibration characteristics of dislocations.

The importance of this subject is due to the major role of dislocations on the plastic deformation of materials. By the improvement of knowledge about the dislocation behaviour, it would be possible to produce more appropriate materials for engineering use.

The model is a two-dimensional, atomistic one. For every atom on the lattice, the governing equation of motion is derived, and it is solved as a function of time, numerically. To perform the calculations, a computer program is used.

The results obtained for several parameters are presented, and a discussion about the results is included. At the end of the thesis, a list of recommendations for a continuation of this study is given.

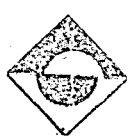

ÖZET

Bu tezde, kenar tipi dislokasyonların hareket ve titreşim karakteristikleri incelenmektedir. İçerilen konular kesme kuvveti-dislokasyon hızı bağıntısı, model parametrelerinin ve iç sürtünmenin dislokasyon hareketi üzerindeki etkileri, dislokasyonun çeşitli engeller arasındaki hareketi, bağlı dislokasyonların titreşim karakteristikleri ve sıcaklık, sürtünme ve geometrik parametrelerin dislokasyon titreşim karakteristikleri üzerindeki etkileridir.

Bu konunun önemi, dislokasyonların, malzemelerin plastik şekil değiştirmelerinde en önemli etken olmalarından kaynaklanmaktadır. Dislokasyon hareketi hakkında bilgilerin artması da amaca uygun malzeme seçiminde ve hatta üretiminde faydalı olacaktır.

Kullanılan model, iki boyutlu ve atomlardan oluşan bir modeldir. Modelde bulunan her atom için kuvvet denklemi yazılır, ve bu denklemin nümerik metotlarla çözülmesiyle o atomun zamana göre pozisyonu belirlenir. Hesaplamalarda bir kompüter programı kullanılmaktadır.

Çeşitli parametreler için elde edilen sonuçlar ve bunların bir analizi sunulmaktadır. Tezin son kısmında bu tezin devamı olarak yapılabilecek çalışmalar hakkında öneriler verilmektedir.

TABLE OF CONTENTS

ABBREVIATIONS AND SYMBOLS

ABBREVIATIONS

cm : centimetre

gm : gram

s : second

SS : steady state

1-D: one dimensional

2-D: two dimensional

3-D: three dimensional

GREEK LETTER SYMBOLS

γ : the distance from a minimum of the substrate potential to the point of change of curvature (dimensionless)

Δ_s : logarithmic decrement

Δt : time increment

η : damping constant (dimensionless)

λ_S : eigenvalue of stable matrix S

λ_U : " " unstable " U

μ : shear modulus

π : ratio of circumference to its diameter

ρ : density

σ : applied shear stress

σ_P : Peierls stress

σ_{PD} : dynamic Peierls stress

τ_o : period of free vibration

ϕ : dimensional form of γ

ω_o : frequency of free vibration

ROMAN LETTER SYMBOLS

B : damping constant (dimensional)

b : lattice parameter

c_S : transverse wave speed

c_L : longitudinal " "

D : dislocation position column number

E : Young's modulus

E(0): initial energy of the lattice

F(t): energy lost to the medium up to time t

F : substrate force

G : shear modulus

j : row index

j : half cycle number

k : column index

k_1 : linear spring constant

k_2 : shear " "

L : dislocation length

M : a number which determines the number of weak bonds

M : number of columns in the lattice

M_L : limiting iteration number used in the numerical solution of the convolution theorem

m : mass

N : number of rows in the lattice

NN : number of time increments

n : number of iterations

n_w : number of weak bond atoms

P : $k_2/k_1 = G/E$

$Q(t)$: energy lost from the boundaries up to time t

S : stable region, stable matrix

T : temperature

T : kinetic energy of the atoms on the lattice

t : time

U : unstable region, unstable matrix

u : displacement from the equilibrium position

V : substrate potential

V_L : linear spring energy

V_S : shear " "

V_P : substrate potential energy

v : speed of dislocation

v_0 : initial velocity of atoms

v_b : breakdown velocity

v_∞ : speed of wave propagation in the crystal

X_j : integrated velocity at half cycle number j

x : position

$\dot{x}$: velocity

$\ddot{x}$: acceleration

z_k : position of k'th atom in linear chain

LIST OF FIGURES

LIST OF TABLES

CHAPTER I

INTRODUCTION

The perfect crystallinity of materials is disrupted by imperfections of various kinds. These are point defects, line defects, surface defects and volume defects. The major imperfections are point defects (vacancies, interstitials) and line defects (edge dislocations and screw dislocations) . Although these affect a very small fraction of the atoms, they are very important in determining the properties of materials such as strength, hardness and ductility.

An edge dislocation is a linear defect that is responsible for nearly all aspects of the plastic deformation of materials. In order to introduce an edge dislocation in a perfect lattice, an extra half plane of atoms are added to the lattice. (Fig. 1)

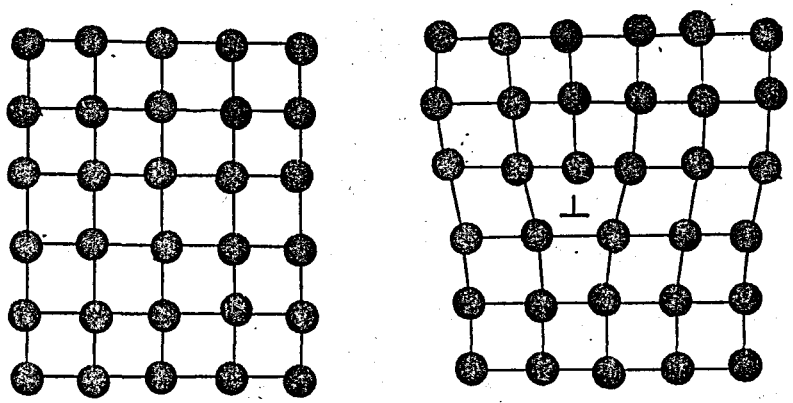

(a) (b)

Fig. 1 Crystal without (a) and with (b) an edge dislocation

The experimental value of the shear stress necessary to move a plane of atoms over another is much less than the value calculated theoretically. (About 1/100 th or 1/1000 th) This discrepancy arises because of dislocations. Fig. 2 shows how an edge dislocation facilitates the motion of one plane over another. Because only one row of atoms must move at any time, and because the row which moves is already in a distorted, energetically unstable position, less force is needed to carry out the shear.

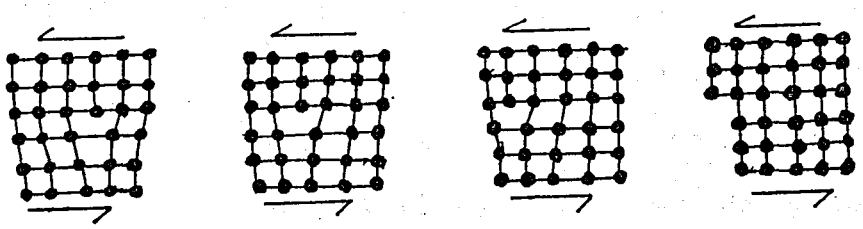

Fig. 2 The motion of an edge dislocation under a shearing stress.

The dynamics of dislocations in crystals has long been a subject of active investigation because of its central role in the plastic flow of crystalline solids as expressed above.

An extensive review of the research done on the subject is given in chapter II.

Most of the research on dislocation behaviour has been done theoretically, because experimental methods for observing dislocations and studying their individual properties, have been developed recently, and it is still difficult to utilize these techniques. (see ref. [1,2,3]).

Theoretical treatments of the problem have been made on the basis of purely continuum models, combined continuum and atomistic models and on purely atomistic models.

Most of the theoretical analysis have been based on continuum models, using linear (isotropic or anisotropic) elasticity. [4] , [5]

While these continuum treatments have provided valuable insight to the problem, the use of atomistic approach became more attractive because of the discrete nature of the lattice itself. After 1970's, high speed digital computers enabled the use of numerical methods, so it became possible to simulate more realistic models, even in three dimensional (3-D) form, for the actual crystal.

Atomistic models can be grouped in two broad categories which are complementary in their purpose. The first type is designed with a particular material or a class of materials in mind and is formulated to be as realistic as possible both with respect to crystal geometry and interatomic force laws. When analyzed by computer simulation, these models provide valuable detailed information regarding atomic processes in the given class of materials. Because of their complexity, however, it is difficult to compare the computer simulation studies by analytical treatment of the same models, and dynamical treatment of the dislocation motion in such realistic models, even by computer simulation methods,

would be very costly and have not yet been attempted.

The second category of atomistic models are highly idealized both from the viewpoint of crystal geometry (sometimes taken as one dimensional) and of interatomic force laws. They clearly, therefore, are not intended to represent directly any particular real material. Nevertheless, they do serve to provide insight into these broad features of dislocation motion which are introduced by the discrete atomic character of crystalline materials in general, without entering into the detailed characteristics peculiar to a particular material. Their idealized nature makes the analytical treatment of these models reasonable, if not easily attainable, objective. When treated by computer simulation techniques, their simplicity facilitates extracting significant patterns of behaviour from the numerical results, particularly when computer graphics techniques are employed.

The model used in this study falls into the second category given above. Its details will be explained extensively in chapter IV .

It would be better to discuss the purpose and the importance of this study after making the literature survey of the subject.

CHAPTER II

REVIEW OF THE ATOMISTIC APPROACH

The simplest atomistic model was introduced by Frenkel and Kontorova[6]. The basic element of their theory consists in the longitudinal displacement of a chain of elastically bound atoms over a similar chain which is rigid. They show that this displacement can proceed in a similar way to the motion of a caterpillar, the atoms of the front portion still being in their positions while the atoms of the rear portion have already moved one elementary distance 'b'; the state of the intermediate portion(compression) being propagated along the chain with a definite velocity. The two chains are assumed to be infinite, the atoms of the upper chain lying in the normal position just above the corresponding atoms of the lower chain (Fig. 3).

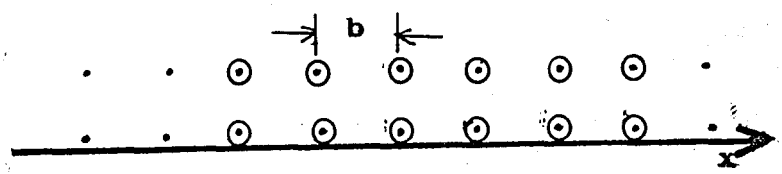

Fig. 3 Upper and lower chain of atoms used in Frenkel-Kontorova approach

If the lower atoms are not rigid, then, this leads to a gradual leak of energy from the upper chain and to a final stopping of process of slip. But if they are treated

as fixed, then, their influence on the upper atoms reduces to the production of a certain periodic field of force.

Now the atoms of the upper chain behave as small spheres lying in their equilibrium places in equidistant valley of a sinusoidal mountain chain and bound to each other by elastic forces, proportional to their relative displacements. (Fig. 4)

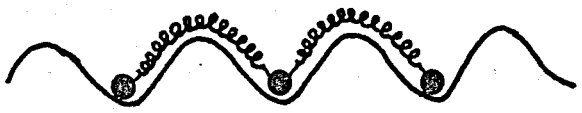

Fig. 4 The conditions of the upper chain atoms

Under these conditions, two types of motion are possible:

1) Small oscillations of the spheres (atoms) about their equilibrium positions,
2) A displacement of each sphere from its original equilibrium position to that formerly occupied by the next.

The second type of motion is regarded as the fundamental mechanism underlying the phenomena of plastic deformation (slip) or twinning.

Under these conditions, Frenkel and Kontorova find the equation of motion for an atom, and by solving it, they conclude that:

1) The velocity of slip propagation is always smaller than the velocity of sound,

2) To every value of the total energy of the system corresponds a definite velocity of slip propagation,
3) In the absence of damping (energy exchange between the chains) a single impulse starting the slip process could lead to a displacement of the whole atomic chain equal to an arbitrary large multiple of the elementary interatomic distance.

This one-dimensional theory can be generalized to two dimensions without any difficulty. The slipping is propagated in this case with a linear front along a definite direction in a given plane (x,y) , the atoms of the underlying plane remaining fixed. Generalization to three dimensions is also possible.

In another paper, Frenkel and Kontorova[6] find a relation between the energy loss of the atomic chain and its total energy when the lower chain is not fixed but the atoms are making small oscillations (damping): The rate of dissipation is high if the total energy is small and it decreases with the increase of total energy. They also give the equation for the distance, travelled by the slip up to the moment of its complete stopping.

In 1962, Sanders[7] made an analytical investigation of the geometry of an edge dislocation in a simple atomic model of an infinite crystal, and the effect on the dislocation of externally applied shear stress. The physical model was a two dimensional lattice, and the variation of dislocation width and Peierls-Nabarro stress

was investigated for some model parameters.

Kratochvil and Indenbom[8] solved the one dimensional Frenkel-Kontorova model with dislocation by changing the sinusoidal substrate potential into a parabolic one so that the substrate force is piecewise linear. They also derived an expression for Peierls stress; cases were found when this stress is equal to zero.

In 1964, a similar study was done by Weiner and Sanders[9], in which the Frenkel-Kontorova model is modified by replacing the sinusoidal substrate force by one which is piecewise linear, and exact solutions are found for the static configuration of the linear chain and for the Peierls stress, σ_p.

As a continuation of this study, Weiner[10] calculated the velocity with which the dislocation will continue to move under stress once it has surmounted the first potential barrier, analytically. The treatment is approximate in that only localized modes of motion (local modes) are included. Some calculations are also made about the dynamic Peierls stress which is the stress required to move the dislocation from one stable equilibrium position to an adjacent one, under quasistatic conditions and in the absence of thermal motion. Analytical results are compared with numerical ones. It is found that the dislocation velocity is a very sensitive function of stress at low velocities, becoming less sensitive to stress when dislocation velocities approximately 0.1 V_∞ are reached, where V_∞ is the speed

of wave propagation for infinite wavelength in the linear chain with the substrate potential neglected.

Weiner [11] examined the effects of thermal motion upon the sustained dislocation motion which was studied in [10] from an athermal viewpoint.

By using the same Frenkel-Kontorova model of a dislocation with a piecewise parabolic potential, Atkinson and Cabrera [12] made some theoretical study on the low and high velocity motion of the dislocation. They concluded that continuum models are not proper for this problem because of the discrete nature of the lattice itself; so they discuss the problem on the simplest possible lattice model of a moving singularity, namely the Frenkel-Kontorova model.

Sanders [13] extended the one dimensional Frenkel-Kontorova dislocation model, with a piecewise linear substrate force to two dimensions to describe the entire slip plane of the dislocation with one kink.

In another paper, Sanders [14] develops a one-dimensional approximation to this two-dimensional lattice model through the use of single chain localized modes. After making almost the same analysis as the previous one ([13]), it is found that all the equilibrium properties are in excellent agreement with the properties of the two-dimensional model, and the computation time is about 1/3000 as long. So, it appears that the same one-dimensional model could be used for more extensive investigations of dislocation behaviour, including dynamic effects.

Hartl and Weiner[15] investigated the dynamics of an edge dislocation in a two-dimensional crystal model. They find an energy loss mechanism which leads to a steady state dislocation velocity when a shear stress is applied to the lattice, and calculate the transient and steady state velocities and the minimum stress necessary to maintain a steady state velocity. They observed the absence of localized mode associated with the stable equilibrium configuration of the model, as opposed to the results for the linear chain.

Earmme and Weiner[16] tested the hypothesis of supersonic motion of dislocation proposed by Ishioka[17] . The result of their study is as follows:

When the dislocation velocity reaches the value 0.94 (for some model parameters), the dislocation breaks down, i.e., the regular dislocation motion exhibited up to that time and postulated in the analytical solution no longer takes place. This velocity is called the breakdown velocity v_b. This is checked by several cross checks and proved to be correct. Their conclusion is that, Atkinson-Cabrera[12] solution does not provide support for the hypothesis that dislocations may be accelerated to supersonic speeds since it ceases to be valid at velocities greater than $v_b < 1$.

In a following study, Earmme and Weiner [18] demonstrated this breakdown phenomena analytically. They also studied the behaviour of the model at stress levels higher than that which causes breakdown, numerically. They found that a growing extended fault is then generated which has highly compressed region in the lead portion and a highly rarefied region in the trailing portion. Under continued stress application, collision waves are generated which travel at supersonic velocities.

Weiner and Pear [19] indicated that breakdown occurs in the case of motion of an edge dislocation in an idealized two dimensional crystal model also, when the dislocation velocity approaches the speed of longitudinal waves.

Perchak and Weiner [20] extended the local mode approximation methods used before in the absence of viscosity to the case in which viscous forces are present. Effect of temperature was examined also.

Another problem is the behaviour of a dislocation when it encounters some obstructions. This subject is first discussed by Frank [21] . In that paper, he states that when a dislocation encounters an obstacle on its path, multiplication of dislocation occurs in the interior of the glide surface by dynamic crassover of dislocations. (Fig. 5)

If the energy of the dislocation at the time of interaction with obstacles, is not high enough to pass

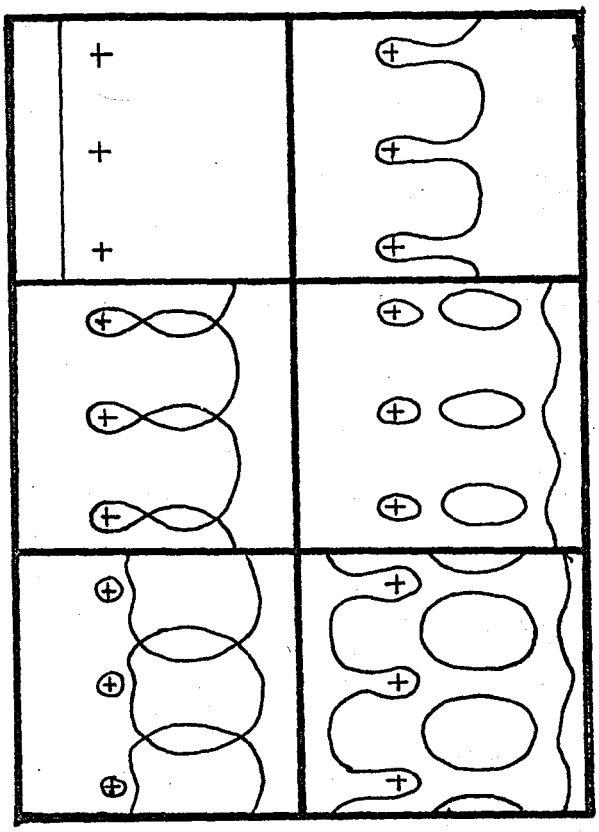

Fig. 5 Multiplication of dislocations[21]

over them by multiplication, it will begin vibrating such as a string fixed at both ends. Then, the damping and other characteristics of the vibration give idea about the internal friction of materials.

This subject was investigated in detail by Weiner et al., [22] in a two dimensional lattice; the following results were obtained: The frequency of free vibration, ω_0, is proportional to the square root of the shear modulus and inversely proportional to the loop length. For the case of model parameters leading to zero Peierls

stress ($\sigma_p = 0$) , the amplitude of dislocation vibration in the atomic model for sufficiently large loop length decays exponentially as in the string model with linear damping. The logarithmic decrement , Δ , of the decay of free vibration is independent of ω_0 .

Weiner et al. [23] extended this model by using a one-dimensional discrete string model and by including additional anharmonicity to the substrate potential. Good agreement was observed between the one and two dimensional models.

Altıntaş [24] compared three different models (continuous string, two-dimensional lattice model and discrete string model) for a pinned dislocation, under an applied stress and when viscous forces are present. It was found that, if the boundary conditions of the 1-D and 2-D discrete lattice models are chosen properly, the results are in close agreement with each other and with the continuous string model.

CHAPTER III

DEFINITION OF THE PROBLEM

When we make an analysis of the subject and the methods used in the investigation of that subject, we see that one of the most important problems in the dislocation dynamics is the motion of dislocations under certain conditions. The basic question discussed to a large extent up to this time is the velocity of the dislocation when the crystal is subjected to a shear stress. What is the applied stress-dislocation velocity relation, what are the effects of the model chosen, initial conditions, viscosity, and other model parameters on the stress-velocity relationship?

In this thesis, the behaviour of the dislocation when it encounters another impurity, such as a fixed atom is also investigated, besides the velocity-stress relation. The last part is about the vibration characteristics of the dislocation when it is fixed at two points, which can be used in obtaining some information about the internal friction of materials.

About the method which will be used in the investigation of the dislocation dynamics; the best one seems to be the atomistic approach with a very simplified and generalized model suitable for the problem. Because, it can be directed to represent any material we want by only changing the model parameters used in the modelling. For

this reason, we used the two-dimensional form of the modified Frenkel-Kontorova model, which was used by Weiner and co-workers [22] . The difficulties arising due to time and data register limitations in computer simulation prevents the use of a 3-D lattice although a 3-D crystal model would give more realistic results. The effect of the third dimension is simulated in the form of a substrate potential field. Even though the use of a 1-D chain would be simpler to handle than a 2-D lattice; the discrepancies between the 1-D and 2-D simulations [15] lead us to use a 2-D lattice.

For each atom on the lattice, the governing equation of motion is derived. These equations are then solved numerically by the addition of necessary initial and boundary conditions, and the position of each atom is determined as a function of time.

A digital computer (UNIVAC 1106) is used in the evaluation of numerical calculations.

Chapter IV explains the model used in the simulation. The results of the calculations are given in Chapters V and VI .

CHAPTER IV

MODEL DESCRIPTION AND THE DERIVATION OF THE EQUATION OF MOTION FOR A SINGLE ATOM

The model used for the computer simulation is based on a simple cubic crystal with nearest-neighbor central and non-central interactions, the so called "Rosenstock-Newell" model [25] , which was used by Sanders [13] , in his atomistic treatment of dislocation kinks in a 2-D form; and by Weiner et al. [22], in the treatment of the vibration of a dislocation fixed at two points after making the necessary modifications

In order to simplify the computer program used in the simulation and to shorten the execution time of each run, only the atoms in the slip plane are treated in detail.

IV.1 Model Description: Consider a three dimensional simple cubic crystal containing a single straight edge dislocation in the [010] direction. Let the slip plane in which the dislocation moves(or vibrates when it is perfectly pinned at equal distances along its length) to be the (001) or x_1x_2 plane. (Fig. 6a)

Only the atoms in x_1x_2 plane are treated explicitly in this simulation. Motion of these atoms are constrained to the x_1 direction so that only force components in that direction need be considered explicitly.

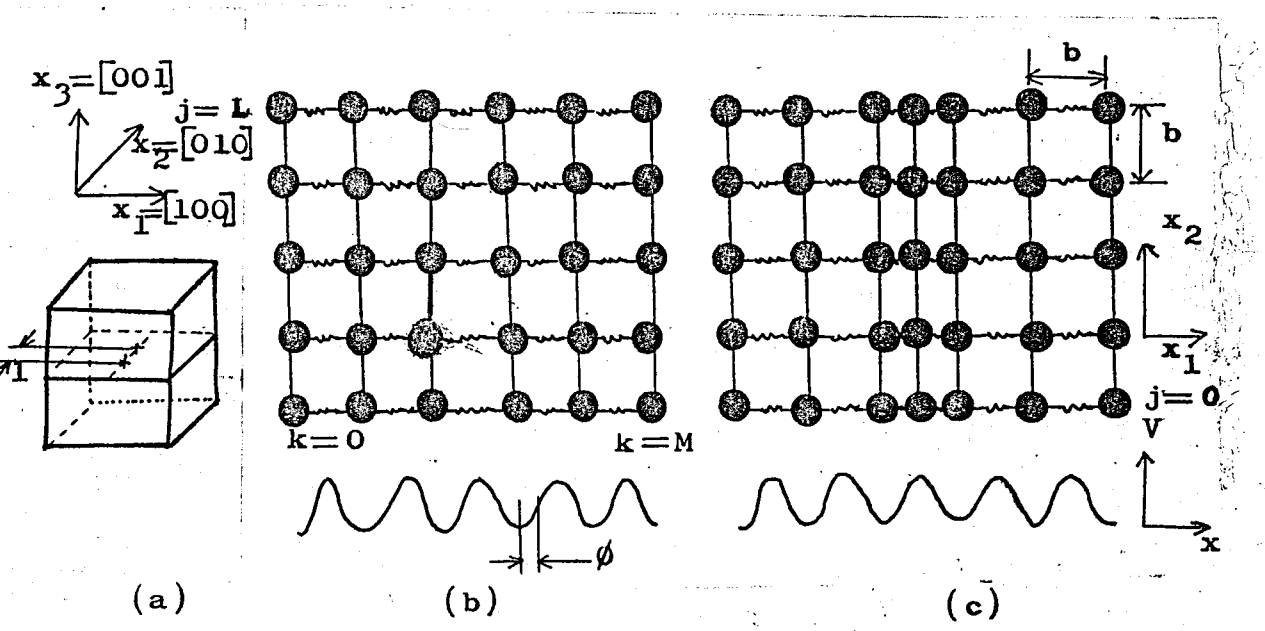

Fig. 6 Model. (a) Simple cubic crystal containing straight edge dislocation. (b) Perfect lattice. (c) Lattice with a dislocation.

The effect of the rest of the crystal is simulated by requiring each slip-plane atom to move in a periodic substrate potential, or force field. That substrate potential is chosen to be piecewise quadratic to obtain linear force components in the equation of motion.

IV.2 Substrate Potential:

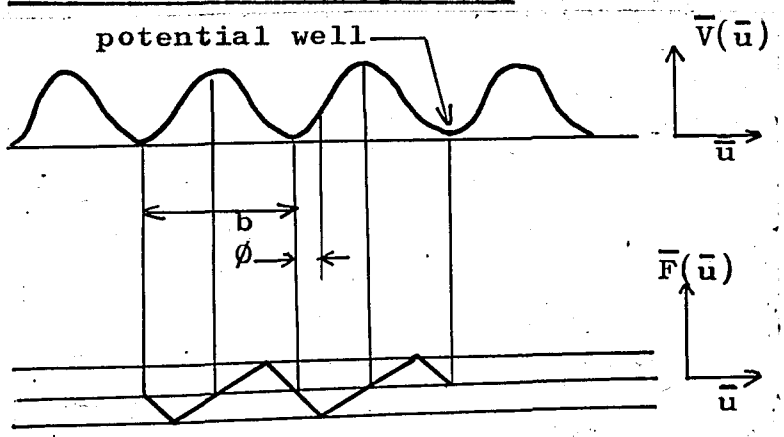

Fig. 7 Substrate potential and substrate force

The force field is a piecewise quadratic one; so the force exerted on every atom , due to that force field, is piecewise linear. (Fig. 7)

The point of intersection of the upper and lower portions of the substrate potential is defined by the distance ϕ from a potential minimum.

If $\bar{u}$ is a displacement of an atom from the nearest potential minimum, then,

substrate potential $\bar{V}$:

$$\bar{V}(\bar{u}) = \begin{cases} \frac{1}{2} k_2 \bar{u}^2 & |\bar{u}| \leq \phi \\ \frac{1}{4} k_2 \phi - \left[k_2 \phi \,/\, (b-2\phi) \right] \left(\frac{1}{2} b - |\bar{u}| \right)^2 & \phi \leq |\bar{u}| \leq \frac{1}{2} b \end{cases}$$

substrate force $\bar{F}(\bar{u}) = -\frac{d\bar{V}(\bar{u})}{d\bar{u}}$, or

$$\bar{F}(\bar{u}) = \begin{cases} -k_2 \bar{u} & |\bar{u}| \leq \phi \\ \frac{2k_2 \phi}{(b-2\phi)} \left(\frac{1}{2} b - |\bar{u}| \right) & \phi \leq |\bar{u}| \leq \frac{1}{2} b \end{cases}$$

where,

k_2 : shear spring constant (noncentral interaction)

b : lattice constant

ϕ : the distance from a potential minimum to the point of change of curvature

IV.3 Lattice with dislocation: In order to introduce a dislocation in a perfect lattice (Fig. 6b) , the number of atoms in one row is kept higher than the number of potential wells. (Fig. 6c) According to the parameters chosen, this difference between the number of atoms in one row and the number of potential wells, defines the number of dislocations in the lattice, and the compatability and stability of the analytical solution of that model. A detailed explanation on this subject is given by Weiner and Sanders[9] . The related parts from that study are given in Appendix A, including the stable and unstable configurations and the Peierls stress.

Here, that difference between the number of atoms and the number of potential wells, is taken to be one; hence, the magnitude of the Burger's vector of the dislocation is one atomic distance, b.

IV.4 Derivation of the Dimensional Equation of Motion: Consider the atom with mass m in the (j,k) coordinate, connected to its nearest neighbors in the x_1 and x_2 directions by springs with linear spring constant k_1 and shear spring constant k_2 respectively. (Fig. 8) $\bar{\eta}$ and $\bar{\sigma}$ represent the phenomenological damping friction constant and the force on the atom due to applied shear stress, respectively. Let $\bar{x}_{j,k}(t)$ denote the x_1 coordinate of the atom in the j'th row and k'th column at time t.

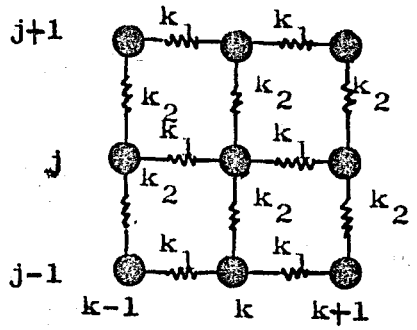

Fig. 8 A single atom with nearest neighbors

Considering a small displacement of the referenced atom, we write the equation of motion using Newton's second law:

$$m\ddot{\bar{x}}_{j,k} + \eta\dot{\bar{x}}_{j,k} + k_1(\bar{x}_{j,k} - \bar{x}_{j,k-1}) + k_1(\bar{x}_{j,k} - \bar{x}_{j,k+1}) + k_2(\bar{x}_{j,k} - \bar{x}_{j-1,k}) + k_2(\bar{x}_{j,k} - \bar{x}_{j+1,k}) = \bar{F}(\bar{x}_{j,k}) + \bar{\sigma}$$

or

$$m\ddot{\bar{x}}_{j,k} = -\eta\dot{\bar{x}}_{j,k} + k_1(\bar{x}_{j,k+1} - 2\bar{x}_{j,k} + \bar{x}_{j,k-1}) + k_2(\bar{x}_{j+1,k} - 2\bar{x}_{j,k} + \bar{x}_{j-1,k}) + \bar{F}(\bar{x}_{j,k}) + \bar{\sigma}$$

Superposed dot is used to denote differentiation with respect to time, as usual. $\bar{\sigma}$ shows the force due to applied shear stress.

IV.5 Derivation of the Nondimensional Equation of Motion: To avoid the difficulties arising from the dimensions of the variables used, we introduce the non-dimensional forms of them.

Introducing the dimensionless variables [20,24]

$$x_{j,k} = \bar{x}_{j,k}/b \qquad Q = 2P\gamma/(1-2\gamma)$$

$$\gamma = \phi/b \qquad t = \bar{t}\,(k_1/m)^{1/2}$$

$$\bar{\sigma} = \bar{\sigma}/(k_2 b) \qquad \eta = \bar{\eta}\,(k_1 m)^{-1/2}$$

$$P = k_2/k_1 \qquad F(x_{j,k}) = \bar{F}(\bar{x}_{j,k})/(k_1 b)$$

using these parameters,

$$F(x_{j,k}) = \begin{cases} -Px_{j,k} & |x| \leqslant \gamma \\ Q(1/2 - |x_{j,k}|) & \gamma \leqslant |x| \leqslant 1/2 \end{cases}$$

$$\frac{d}{d\bar{t}} = (k_1/m)^{1/2}\frac{d}{dt} \qquad \frac{d^2}{d\bar{t}^2} = (k_1/m)\frac{d^2}{dt^2}$$

substituting

$$mb\ddot{x}_{j,k}k_1/m = -\eta(k_1 m)^{1/2}\,\dot{x}\,(k_1/m)^{1/2}b + k_1 b(x_{j,k+1} - 2x_{j,k} + x_{j,k-1}) + k_2 b(\dot{x}_{j+1,k} - 2x_{j,k} + x_{j-1,k}) + \bar{F}(bx_{j,k}) + \sigma k_2 b$$

divide by $k_1 b$

$$\ddot{x}_{j,k} = -\eta\dot{x} + (x_{j,k+1} - 2x_{j,k} + x_{j,k-1}) + P(x_{j+1,k} - 2x_{j,k} + x_{j-1,k}) + F(x_{j,k}) + P\sigma \qquad (1)$$

Nondimensional equation of motion

IV.6 Initial Conditions: It is assumed that initially, at $t=0$, the dislocation line is straight in the x_2 direction, and is in the edge orientation with the extra half plane of atoms, in the upper half of the crystal, ending in the $k=D$ column in the slip plane.

Under these conditions, the initial atomic positions are independent of the row index j, and therefore, there is no interaction between rows. Each row then corresponds to a one-dimensional modified Frenkel-Kontorova of the type treated by Kratochvil and Indenbom[8] and by Weiner and Sanders[9], so that the initial atomic positions may be computed directly from the appropriate formulae which are given in Appendix A, also. The initial positions correspond to the unstable equilibrium positions ($M=3/2$), under zero stress ($\sigma=0$).

Initially all atoms are at rest, that is, the initial atomic velocity of each atom is zero.

IV.7 Boundary Conditions: Since it is assumed that the motion of each segment of dislocation line (Fig. 6_a) is equivalent, the following relations apply for $t \geq 0$ and all k.

$$x_{L+1,k} = x_{L-1,k}$$
$$x_{-1,k} = x_{1,k} \qquad (2)$$

In the x_1 direction, the strip is taken as infinite. In order to simulate this property, localized character of the dislocation motion is used; for atom columns sufficiently far from the dislocation line,

i) atomic positions $x_{j,k}$ are independent of k; interactions between rows may be neglected,

ii) atomic displacements remain near the bottom of their respective potential wells and do not exceed γ in magnitude; the linearity of the equations of motion, governing the atoms in the exterior regions, is ensured.

Therefore, the displacement $u_{j,M+1}$ of the j,M+1 atom from the bottom of its well may be expressed in terms of the corresponding displacement $u_{j,M}$ by means of the convolution theorem. [22]

First consider a semi infinite chain with defining equation:

$$\begin{aligned} &\ddot{z}_k = z_{k+1} - (2+P)z_k + z_{k-1} - \eta \dot{z}_k && k \geqslant 0 \\ &z_k(0) = \dot{z}_k(0) = 0 && t = 0\ ,\quad k \geqslant 0 \\ &z_0(t) = 1 && t > 0 \end{aligned} \qquad (3)$$

Then, by convolution theorem,

$$u_{j,M+1}(t) = \int_0^t u_{j,M}(t-\tau)\dot{z}_1(\tau)d\tau \qquad a$$

$$u_{j,-1}(t) \quad \int_0^t u_{j,0}(t-\tau)\dot{z}_1(\tau)\, d\tau \qquad b \qquad (4)$$

The relevant atom positions may be obtained from the corresponding atom displacements by the following relations:

$$x_{j,-1} = u_{j,-1} - 1 \qquad x_{j,0} = u_{j,0} \qquad (5)$$

$$x_{j,M} = u_{j,M} + (M-1) \qquad x_{j,M+1} = u_{j,M+1} + M$$

IV.8 Finite Difference Approximations: For the numerical solution of the equation of motion (1), finite difference approximations are used:

$$\ddot{x}^n_{j,k} \cong (x^{n+1}_{j,k} - 2x^n_{j,k} + x^{n-1}_{j,k}) / (\Delta t)^2 \qquad (6)$$

$$\dot{x}^n_{j,k} \cong (x^{n+1}_{j,k} - x^n_{j,k}) / (\Delta t) \qquad (7)$$

n is the iteration number at time t ($n = t/\Delta t$)

Substitution of equation (6) into equation (1) permits the computation of $x^{n+1}_{j,k}$ in terms of $x^n_{j,k}$ and $x^{n-1}_{j,k}$. The computation is begun by utilizing (7) with the prescribed initial configuration $x^0_{j,k}$ and taking $\dot{x}^0_{j,k} = 0$ in order to compute $x^1_{j,k}$.

The convolution integrals of (4) are evaluated numerically, in the following manner: For a given choice of Δt, the problem corresponding to equation (3) is solved numerically, using the finite difference equations (6) and (7), and the values of $z_1^n = z_1(n\Delta t)$ are stored. Then, equation (4a) is approximated as

$$u^n_{j,M+1} \sum_{m=1}^{n} u^{n-m}_{j,M} (z_1^m - z_1^{m-1}) \qquad (8)$$

A similar approximation is used for (4b). For a sufficiently large m, $m > M_L$, the difference $z_1^m - z_1^{m-1} \cong 0$. It is therefore necessary to store z_1^m only for $m \leqslant M_L$ and permissible to truncate the sum in equation (8) at M_L for $n > M_L$.

CHAPTER V

SIMULATION RESULTS

V.1 Dynamic Peierls Stress: In order to calculate the dynamic Peierls stress of the dislocation, the procedure given in Appendix A was followed: For a given η, a stress σ was chosen, and iteration was begun by the use of initial and boundary conditions. Since the initial atomic configuration does correspond to unstable configuration, following Appendix A, we can conclude if the applied stress σ is higher than the dynamic Peierls stress σ_{PD} or lower than it, by only observing if the dislocation moves or it cannot pass over the first potential barrier. This procedure was continued by increasing σ if the dislocation does not move, or by decreasing σ if the dislocation moves, until σ_{PD} was obtained.

The parameters used in the calculations:

M : 41 lattice column number or lattice width

N : 5 " row " " " height

P : 0.5

γ : 0.3

σ_{PD} obtained for two different η values are:

η : 0.1 σ_{PD} : 0.0038

η : 0.2 σ_{PD} : 0.0068

V,2 Dislocation Velocity: To determine dislocation velocity as a function of time, a stress $\sigma \geq \sigma_{PD}(\eta)$ was chosen, and the simulation was allowed to proceed until a steady-state (SS) condition for the dislocation motion was reached. As a measure of dislocation velocity, three different approximations were used:

1) $$v(t)=\frac{1}{N}\sum_{k=1}^{M}\sum_{j=1}^{N}\dot{x}_{j,k}(t)$$

2) $$v(t)=\frac{1}{tN}\sum_{k=1}^{M}\sum_{j=1}^{N}\left[x_{j,k}(t)-x_{j,k}(0)\right]$$

3) $$v(t)=\frac{1}{t}\sum_{k=1}^{M}\left[x_{jN,k}(t)-x_{jN,k}(0)\right]$$ jN: middle row

Here, the first approximation is the instantaneous velocity of the dislocation, whereas the second and third ones are time averaged velocities. In the second approximation, all of the atoms are taken into consideration, but in the third one only the middle row is included.

It was observed that, the second and third approximations for the dislocation velocity give exactly the same result, showing the dislocation remains straight during motion, unless the lattice contains an impurity. The instantaneous velocity fluctuates much at the beginning, differing from the other two velocities to a large extent; but as the SS velocity is approached it takes almost the same value of other two approximations.

Fig. 9 shows a typical dislocation velocity vs. time curve.

Parameters used:

P : 0.5

γ : 0.25

η : 0.1

M : 41

N : 3

σ : 0.0050

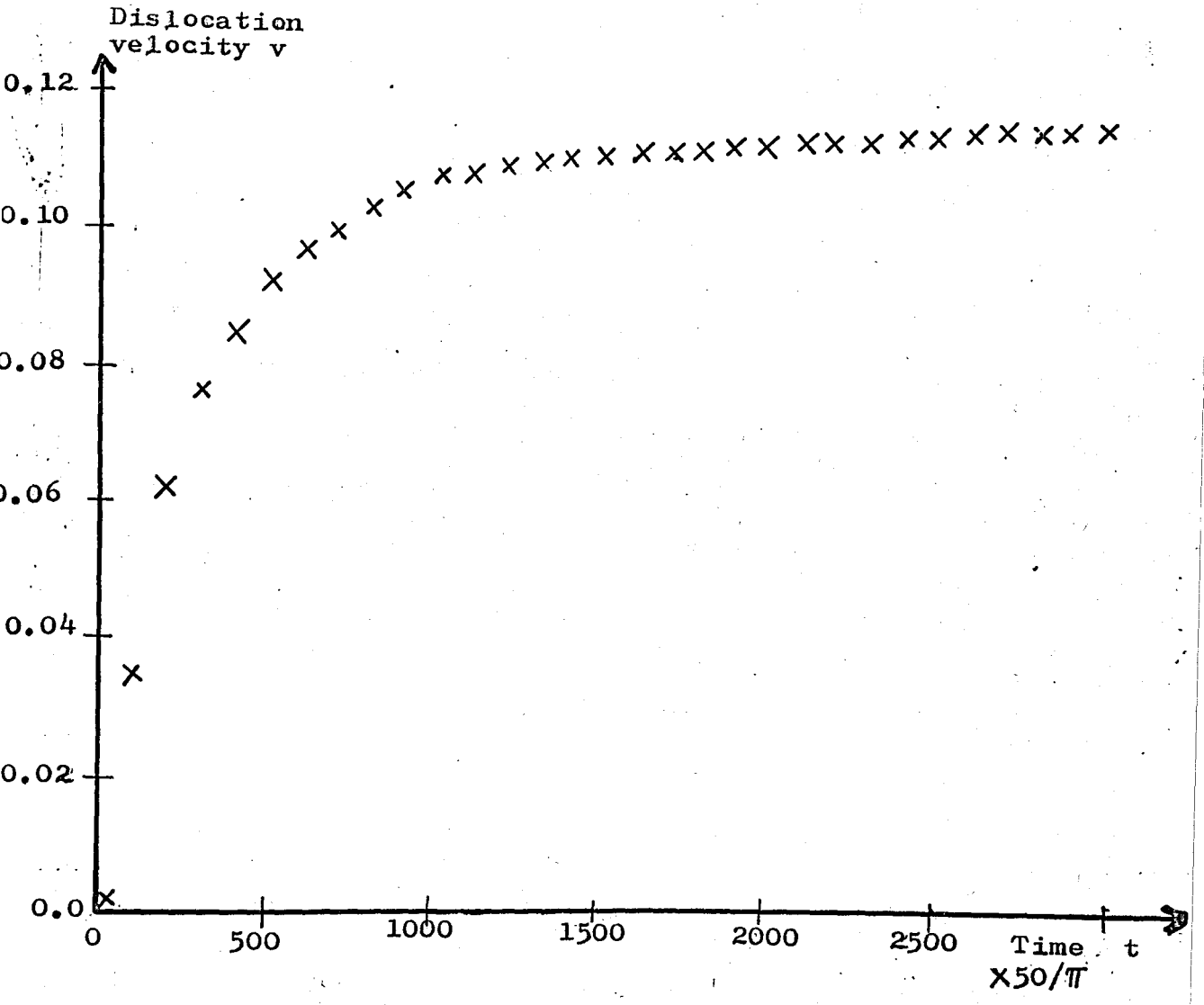

Fig. 9 A typical dislocation velocity vs. time curve

V.3 Dislocation Velocity for Nonzero Peierls Stress:

In Appendix A, it is explained that , for a given value of n_w (the number of weak bond atoms) , σ_p can be calculated as a function of P and γ.

For $n_w = 1$, the relation between P and γ which corresponds to $\sigma_p = 0$ is

$$\gamma = \frac{1}{4}\left[P + 2 - (P^2 + 4P)^{1/2}\right]$$

When γ is not chosen according to this relation, Peierls stress exists for the model, and its magnitude may be calculated by following the formulations in Appendix A. (Fig. A2)

Some runs were evaluated to see the effect of applied stress σ on steady dislocation velocity v, when Peierls stress exists. To compare the results with the one dimensional calculations of Perchak and Weiner [20] , $P = 0.5$ and $\gamma = 0.3$ were chosen. For these parameters, the Peierls stress, $\sigma_p = 1.42 \times 10^{-2}$

The steady state dislocation velocities for $\eta = 0.0$, 0.1 and 0.2 are shown in Fig. 10

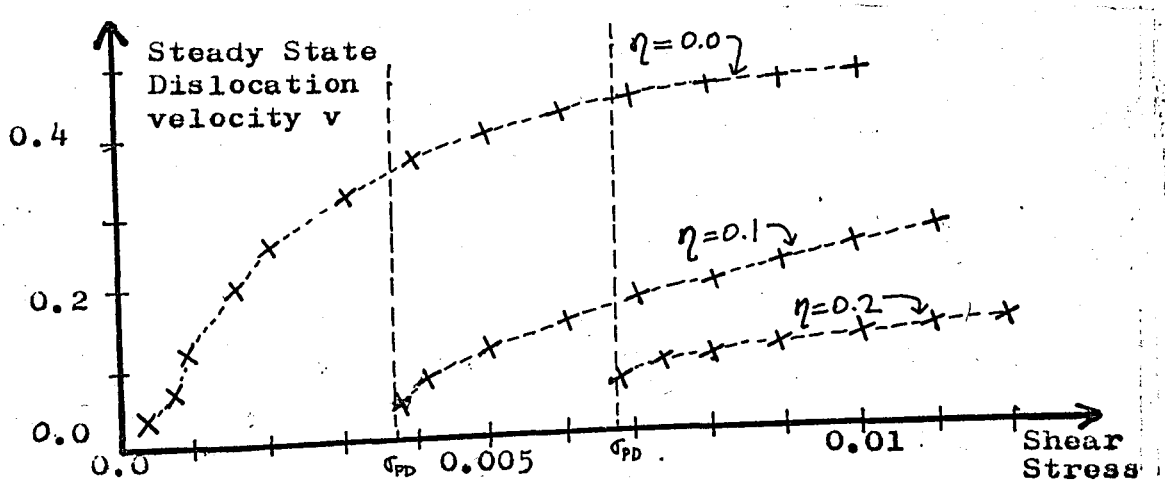

Fig. 10 Stress dependance of dislocation velocity for nonzero Peierls stress

V.4 Dislocation Velocity vs Peierls Stress: The effect of the Peierls stress on the SS dislocation velocity was investigated by changing γ while keeping P constant for an applied stress $\sigma < \sigma_{PD}$. The results are seen on Table 1.

Parameters used:

P : 0.5

M : 41

N : 3

η : 0.1

σ : 0.0075

Run number	γ	$\sigma_p \times 10^2$	v
1	0.2500	0.00	0.178
2	0.2525	0.10	0.172
3	0.2550	0.25	0.168
4	0.2650	0.65	0.161
5	0.2750	1.03	0.165
6	0.3000	1.42	0.192
7	0.3100	1.30	0.187
8	0.3200	0.93	0.168

Table 1 Dislocation velocity vs Peierls stress

V.5 Dislocation velocity for zero Peierls stress:

For some combinations of P and γ , Peierls stress vanishes. Some runs were evaluated to see the effect of the applied stress σ on the SS dislocation velocity. Parameters used and results obtained are given on Tables 2 and 3 .

$\eta = 0.0$		$\eta = 0.1$		$\eta = 0.2$	
σ	v	σ	v	σ	v
0.0003	0.041	0.0003	0.0073	0.0003	0.0040
0.0010	0.095	0.0010	0.0256	0.0025	0.0352
0.0017	0.131	0.0020	0.0512	0.0050	0.0695
0.0024	0.270	0.0030	0.0756	0.0075	0.1027
0.0030	0.315	0.0040	0.0971	0.0100	0.1315
0.0040	0.369	0.0050	0.117	0.0125	0.1652
0.0045	0.390	0.0075	0.178		
		0.0100	0.247		
		0.0125	0.305		

P : 0.5 γ : 0.25 M : 41 N : 3

Table 2 Dislocation velocity for zero Peierls stress at different damping constants

σ ↓ P →	0.3	0.4	0.5	0.6	0.7
0.0003	0.039	0.039	0.041	0.044	0.047
0.0010	0.093	0.092	0.095	0.101	0.109
0.0017	0.163	0.156	0.131	0.123	0.128
0.0024	0.249	0.265	0.270	0.264	0.138
0.0030	0.292	0.306	0.305		0.327
0.0040	0.341	0.357	0.369	0.378	0.385

M : 41 N : 3 σ_p : 0.0 η : 0.0

Table 3 Dislocation velocity for zero Peierls stress at different P values

Results given on Table 2 are drawn in Fig. 11

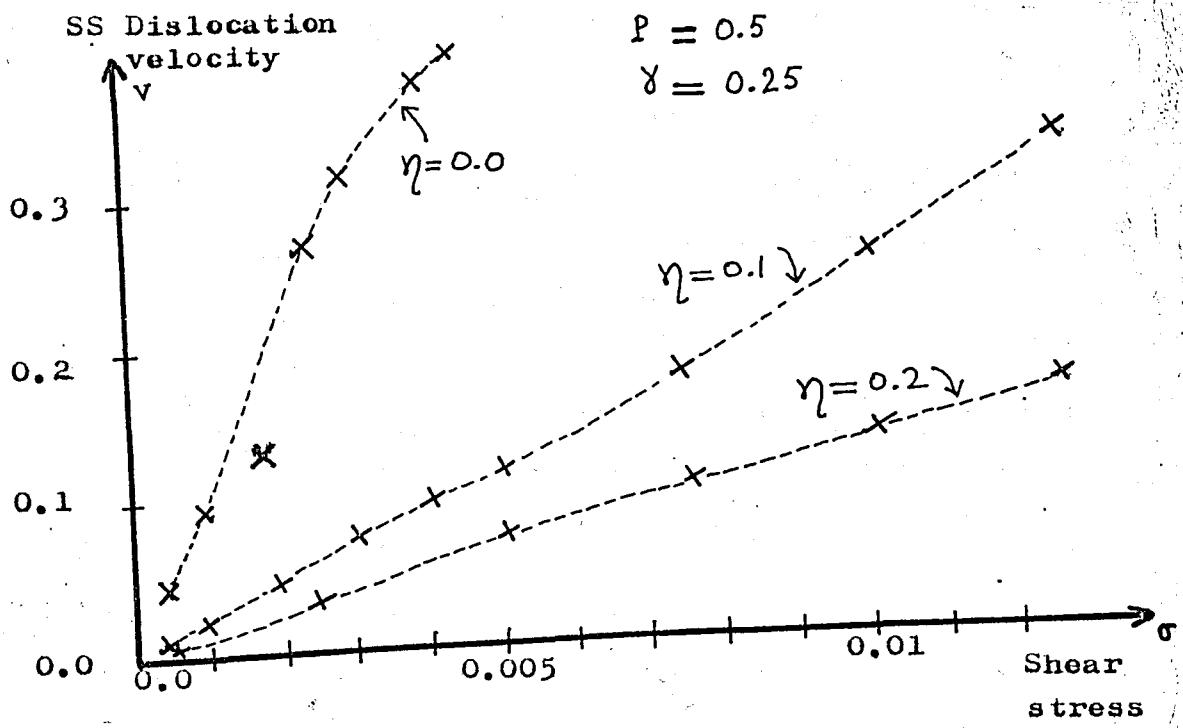

Fig. 11 Stress dependance of SS dislocation velocity for $\sigma_p = 0$

V.6 Movement of the dislocation in the Substrate Potential Field: To examine the analogies given in Appendix A, the instantaneous velocity of the dislocation at the beginning of the motion is given as a function of time in Fig. 12

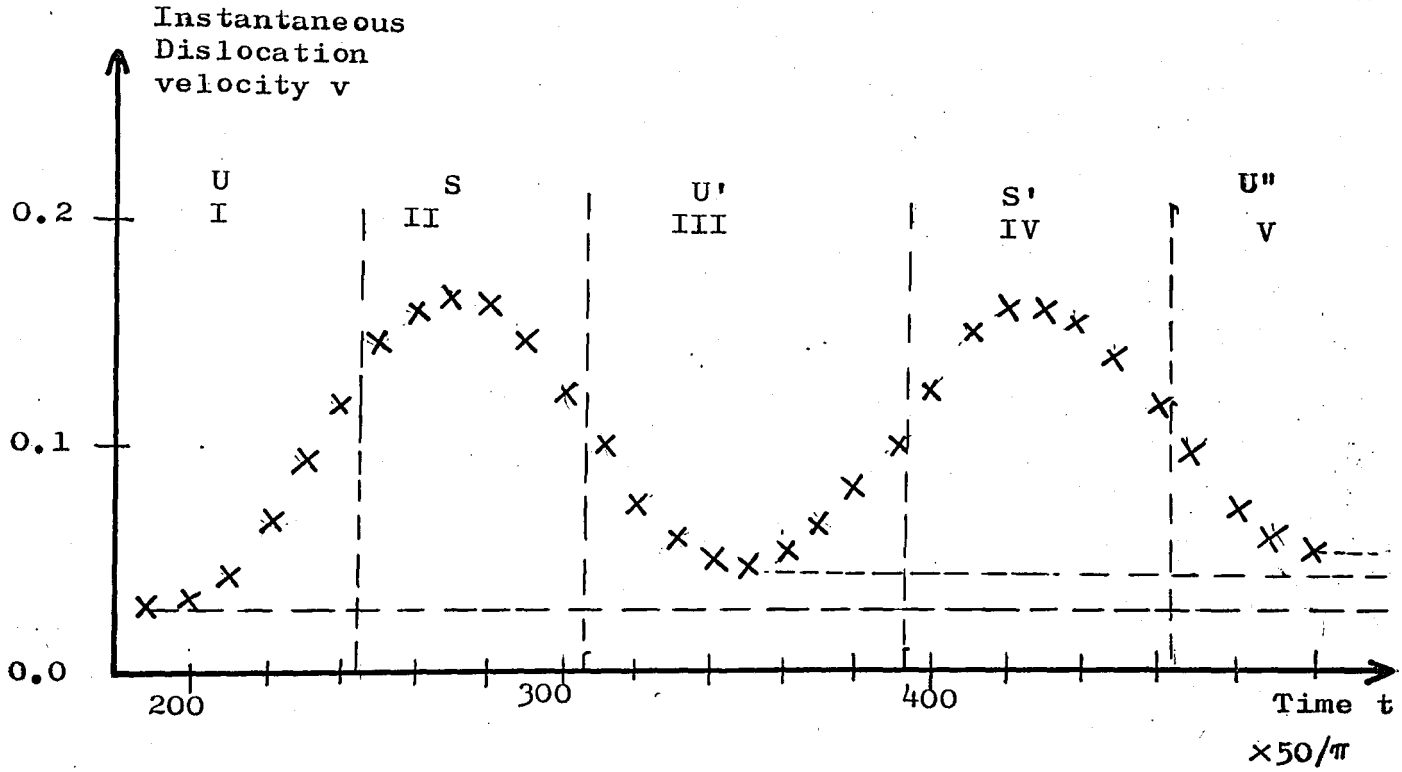

M : 41, N : 3, P : 0.5, γ: 0.3, η: 0.2, σ: 0.0085

Fig. 12 Instantaneous dislocation velocity vs time for $\sigma_p \neq 0$

Region I : Two weak bond atoms (6-7), U (unstable)

Region II : One " " " (7), S (stable)

Region III: Two " " " (7-8), U'

Region IV : One " " " (8), S'

Region V : Two " " " (8-9), U"

Numbers in paranthesis show the column number of weak bond atoms

The velocity of the dislocation is maximum when it is almost at the middle of the stable region, and minimum at the middle of the unstable region. This result is in good agreement with the analogies given in Appendix A.

Note that the instantaneous velocity values, at which the curve is minimum, increases as time goes on, so does the maxima. As the dislocation velocity reaches SS value, that increase in the minima and maxima ends.

It was also observed that the regions II and IV becomes narrower and narrower as the Peierls stress decreases; if $\sigma_p = 0$, those regions vanish, pointing that we have UU' motion instead of USU' motion which is assumed initially in the analytical solution. (see Appendix A)

Fig. 13 shows the variance of instantaneous velocity vs time for similar parameters except $\gamma = 0.25$, resulting

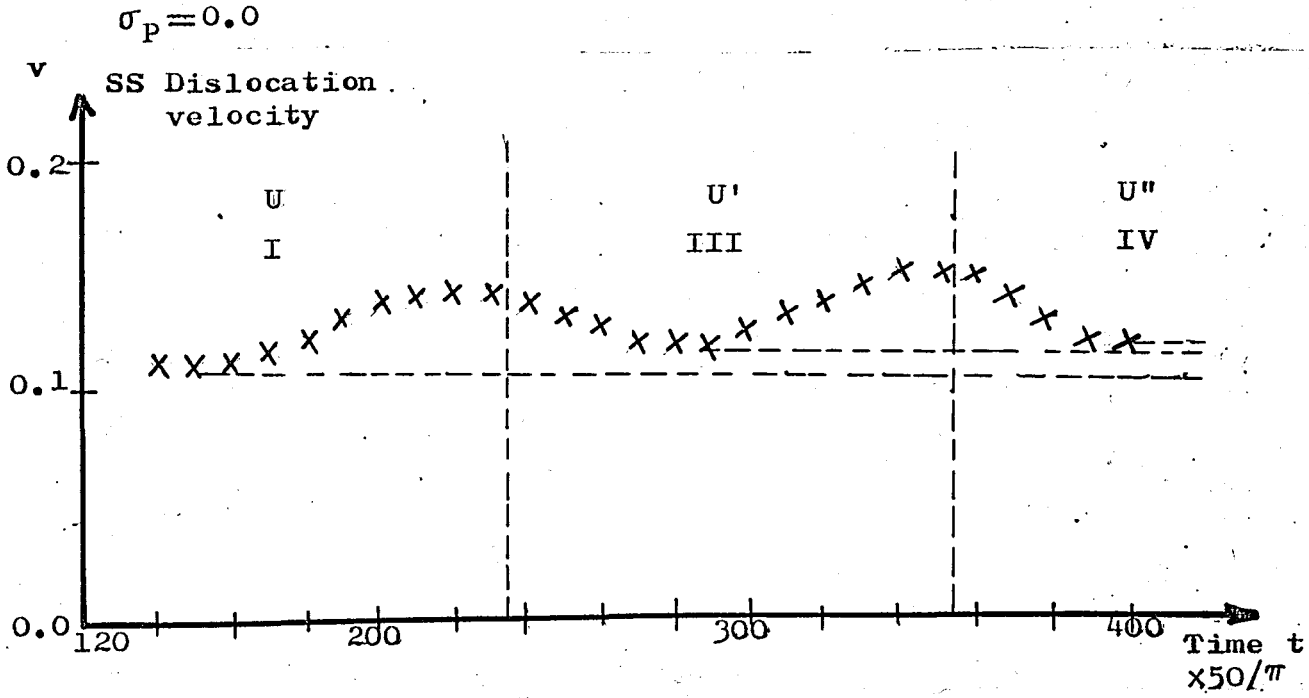

M: 41, N: 3, P: 0.5, γ:0.25, η: 0.2, σ: 0.0100

Fig. 13 Instantaneous dislocation velocity vs time for $\sigma_p = 0$

V.7 Dislocation Position: Position of the dislocation was calculated by using the following formulae:

$$1)\quad r(t) = \left(\sum_{k=1}^{M} \sum_{j=1}^{N} \left[x_{j,k}(t) - x_{j,k}(0) \right] \right) \times \frac{1}{N}$$

$$2)\quad r(t) = \sum_{k=1}^{M} \left[x_{jN,k}(t) - x_{jN,k}(0) \right]$$

These are obtained by multiplying the time averaged dislocation velocities by time.

When there is no obstruction, these two approximations give exactly the same results for the position of the dislocation.

Fig. 14 shows a typical dislocation position vs time curve.

Parameters used:

P : 0.5, : 0.25, M : 41, N : 3, η: 0.1, σ: 0.0050

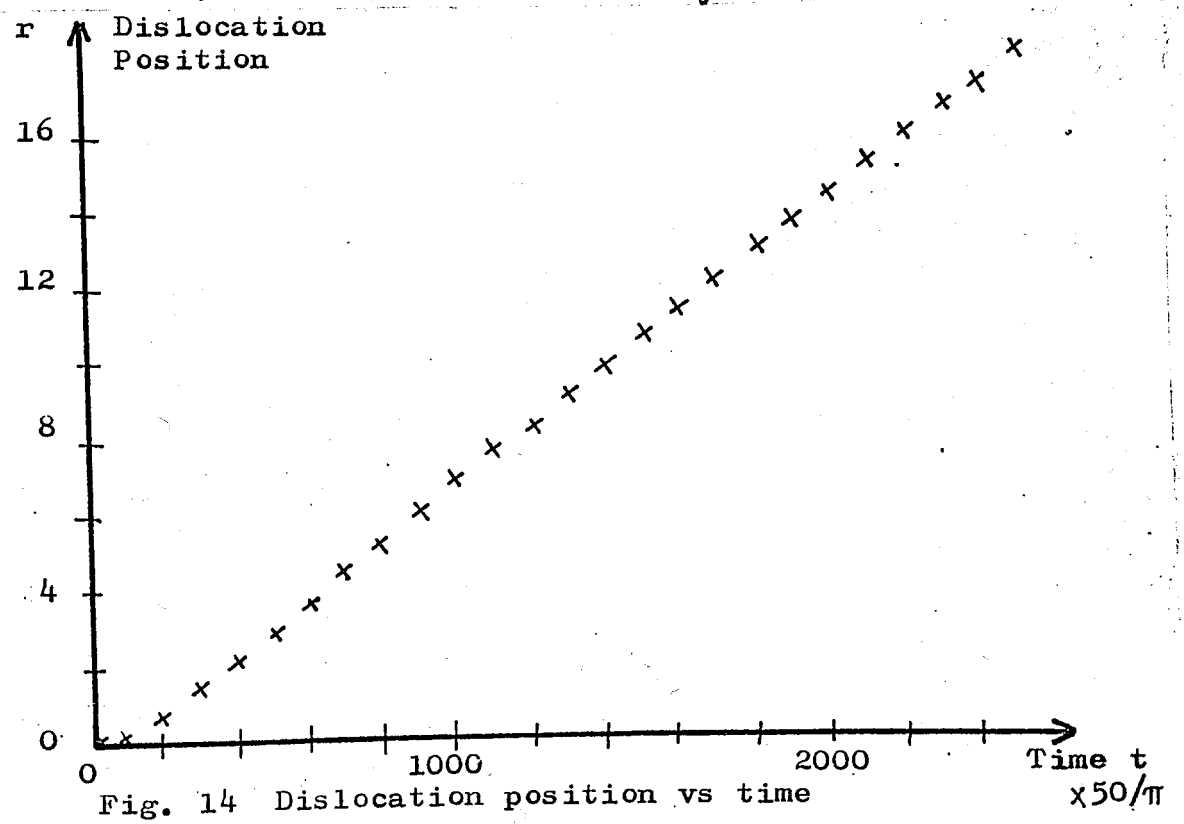

Fig. 14 Dislocation position vs time

V.8 Motion in a lattice with an obstruction: The hypothesis of "multiplication of dislocations", proposed by Frank [21], which is explained in chapter II also, was examined by fixing an atom on the path of the dislocation. The configuration and parameters are as follows:

M : 33 lattice width

N : 11 " height

P : 0.5
γ : 0.25
} $\sigma_p = 0.0$

η : 0.1

σ : 0.0050

Dislocation is at 4.5 atomic distance from left

Fixed atom row number j = 6

Fixed atom column number k=26

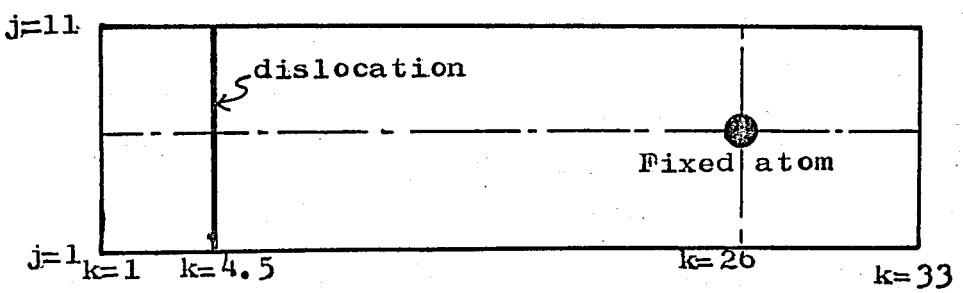

Fig. 15 Lattice with dislocation and a fixed atom

Equations for the fixed atom:

$$\left.\begin{aligned} x_{j,k}(t) &= x_{j,k}(0) \\ v_{j,k}(t) &= 0.0 \end{aligned}\right\} \text{ fixed atom}$$

Fig. 12 shows that the SS velocity $v=0.116$ for these parameters if there were no obstruction.

Until $t=136$, the dislocation motion is normal with a time averaged velocity of 0.115 and a dislocation position of 20.3. There is only a slight difference (around the order of 1/10000), between the time averaged velocities (or the positions) of the dislocation, calculated by including all of the atoms or only the atoms at the middle row. The velocity of the middle row is less than the total velocity, and the dislocation takes a curved shape with the dislocation at the center row is behind the dislocation line at the end rows. After $t=150$, the instantaneous velocity begins to decrease and becomes zero at $t=178$. Fig. 16 shows the decrease of the instantaneous dislocation velocity with time.

After $t=178$, the dislocation velocity becomes negative, which is an indication of a bowing and reflection around the fixed atom. After making some oscillations, the dislocation is almost stopped at $t=325$. The last position of the dislocation at the middle row is 23.66 .

Fig. 17 shows the change of dislocation position with time.

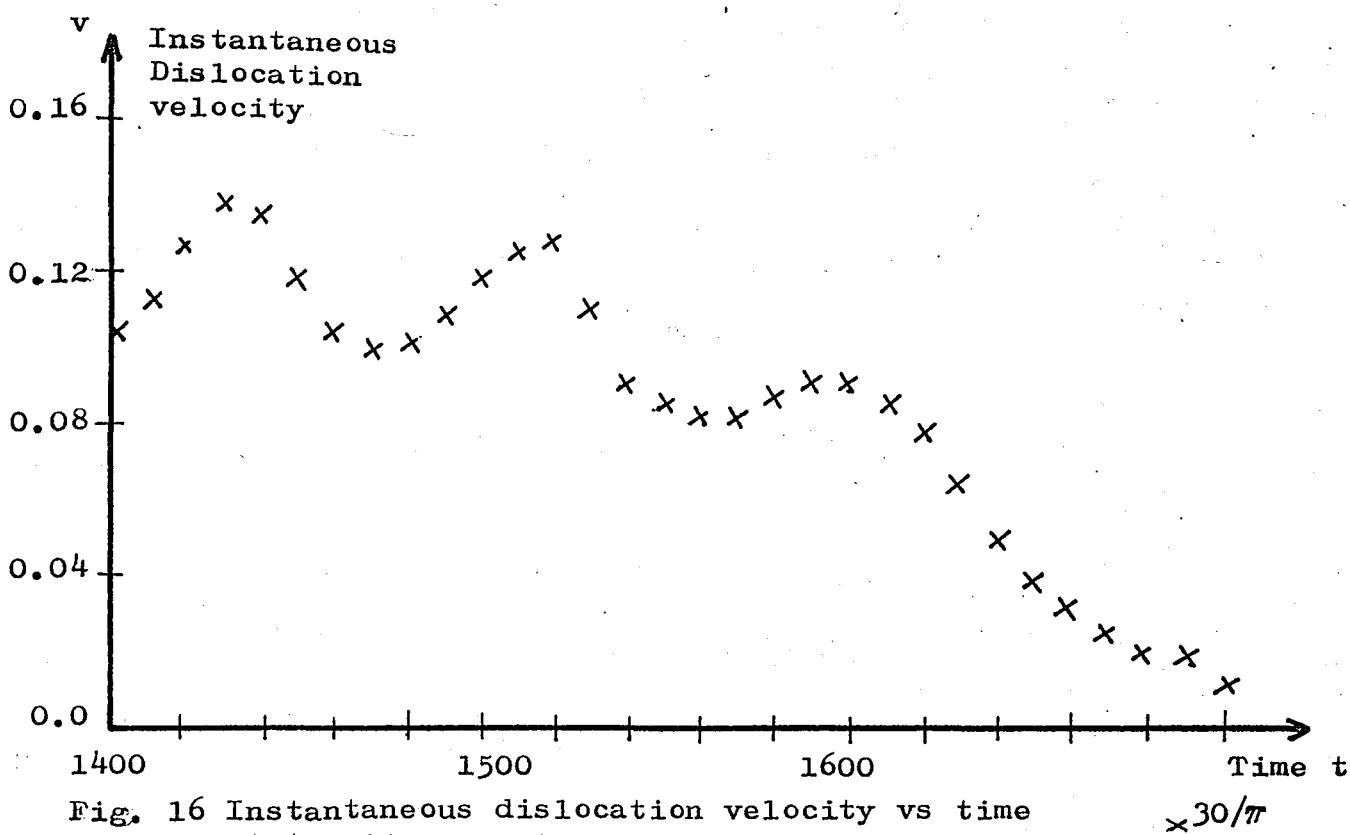

Fig. 16 Instantaneous dislocation velocity vs time at the time of stopping

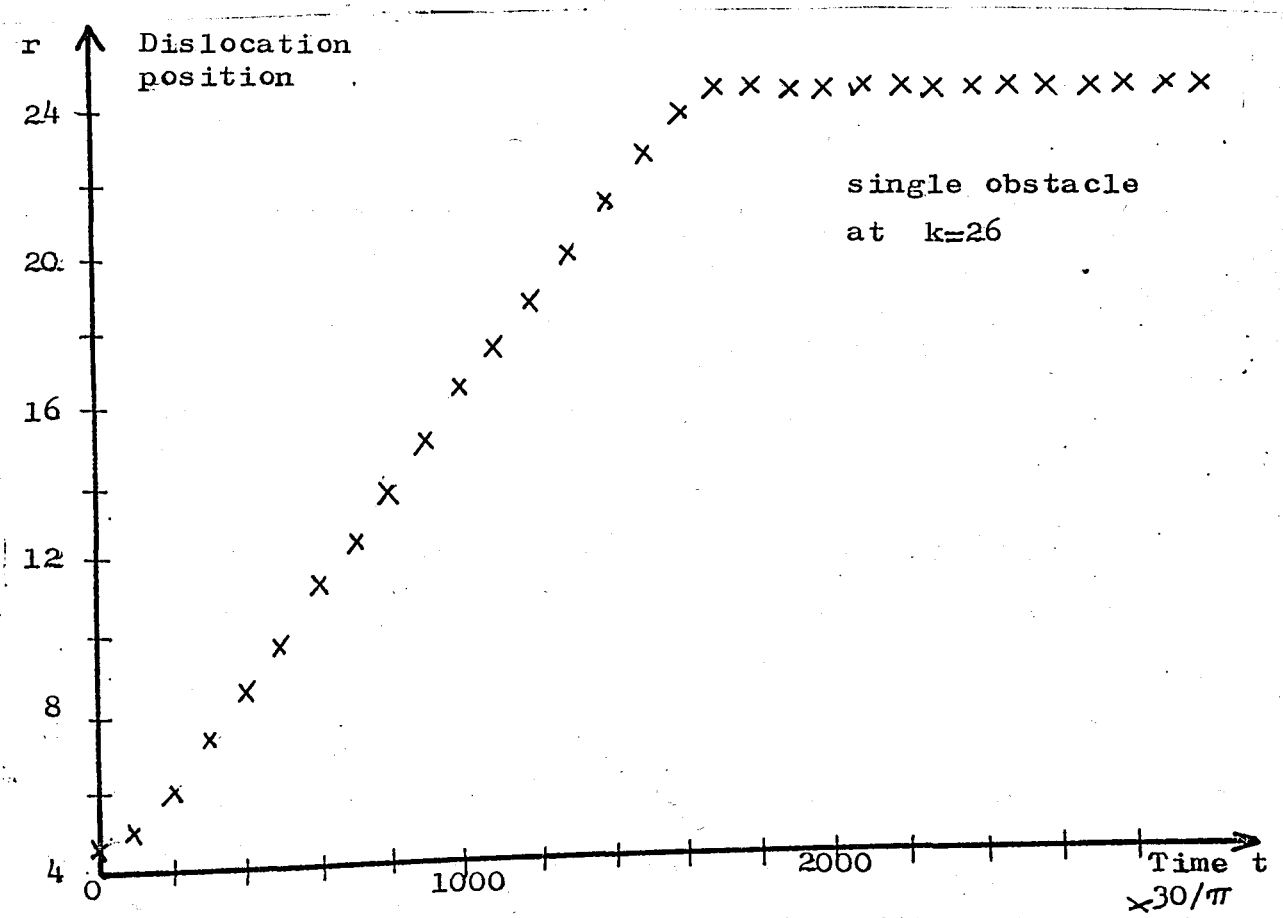

Fig. 17 Dislocation position vs time with obstacle

By the use of Fig. 17, we can draw a velocity vs. time curve for the dislocation. (Fig. 18)

In Fig. 18, the time increment used in the calculation is $10 \times \pi / 3$.

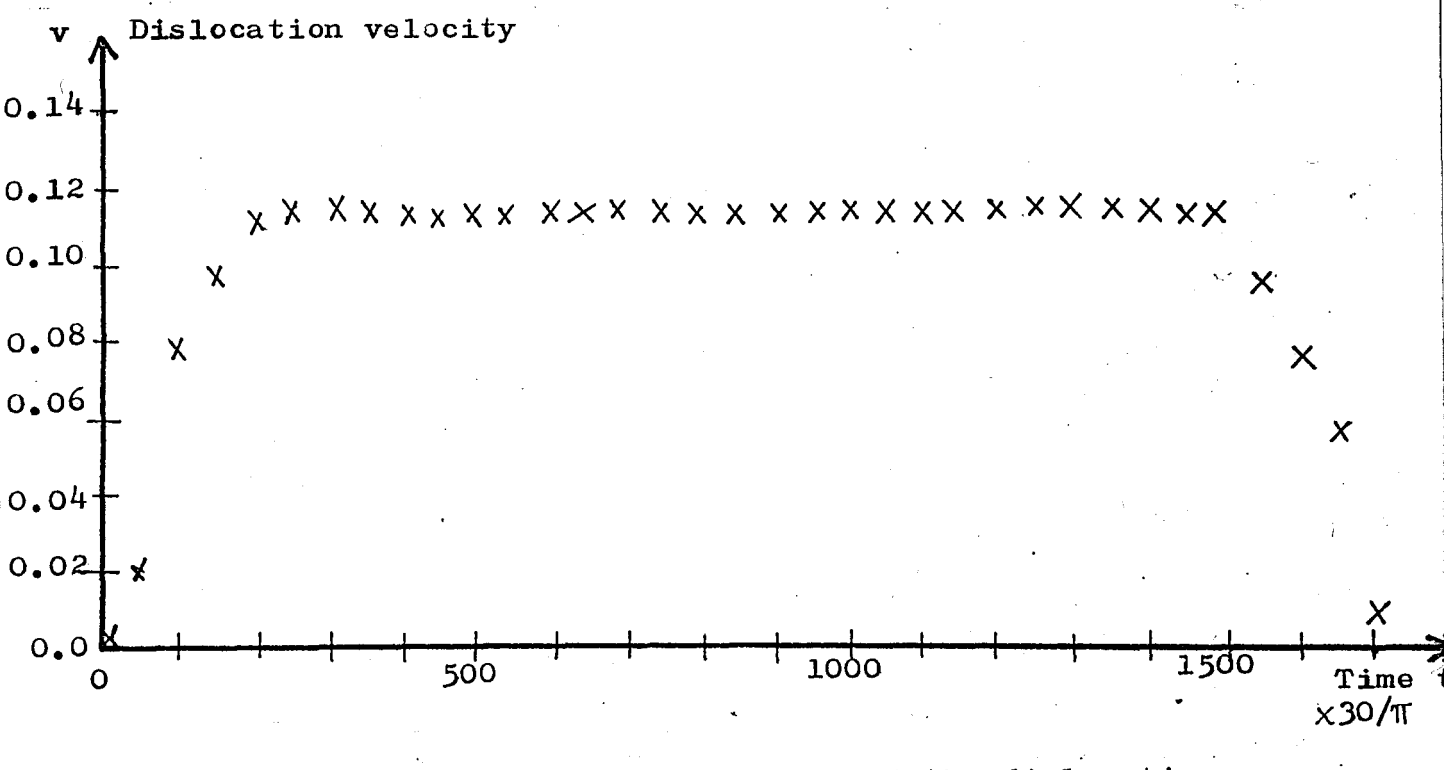

Fig. 18 Velocity vs time graph of the dislocation, when there is an obstruction on the path of it

In another simulation, 2 points were fixed, with row numbers j=1 and j=11. Other parameters are the same as the parameters of the preceeding one.

It was observed that the decrease of the instantaneous velocity is very similar to that one. Only difference is that the position of the dislocation at the

middle row is now ahead of the dislocation at the time of stopping.

The dislocation configuration at t=356 is as follows,

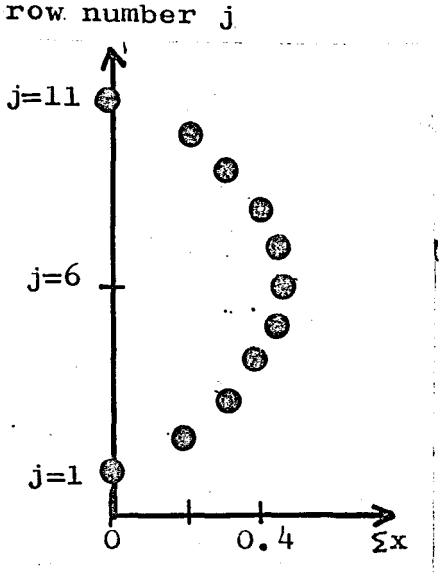

Fig. 19 Final configuration of dislocation

Then, due to the energy stored in the springs, instantaneous velocity becomes negative, showing that the dislocation is moving left. But after some time, the dislocation stops again and moves to the right, because the shear stress σ is still being applied. As a consequence of these motions, dislocation becomes vibrating as if a string fixed at both ends. This vibration ends when the energy of the dislocation is lost completely by the effect of phenomenological damping η.

Several computer runs were carried out in order to determine the characteristics of the dislocation vibration, and they are outlined in chapter VI.

CHAPTER VI

VIBRATION OF A PINNED DISLOCATION

This subject was investigated in detail by Weiner, et al [22] , and several important results were obtained.

It is possible to utilize the computer program used in dislocation motion, in the study of vibration characteristics of dislocations, after making necessary modifications. By doing so, the modified program was used first to obtain results as Weiner et al have obtained, and we found the same results. Then, the program was extended to include damping.

VI.1 Model Description: The same model described in chapter IV was used, except the items given below:

1) Initial Configuration: Initial positions of atoms correspond to the stable atomic configuration for M=1 and σ=0 case. (see Appendix A)

2) Initial velocity: It is difficult to investigate the vibration of dislocations when an external shear stress is applied to the atoms. This difficulty is eliminated by choosing this stress to be zero. In order to initiate the vibration, all atoms are given an initial velocity $v_{j,k}(0)$. Now, the problem becomes simpler; we have free vibration of the dislocation, instead of forced vibration.

Initial velocity distribution:

$$\dot{x}_{j,k} = v_0 \beta^{-|k-D|} \sin\left(\frac{j\pi}{L}\right)$$

where,

v_0 : maximum initial velocity

j : row number of any atom

k : column " " " "

D : column number of dislocation

L : dislocation length (atomic distance between fixed atoms)

$\bar{\beta}$: $1/2\ (\bar{P} + 2 - (\bar{P}^2+4P)^{1/2})$

$\bar{P}$: $P + \lambda$

λ : $2 + P - \left[(P+Q)^2 + 4\right]$

Q : $2P\gamma\ /(1-2\gamma)$

This initial atomic velocity distribution specifies:

a) a sinusoidal variation in j direction,

b) the lowest frequency localized mode of vibration in the stable configuration, in the k direction. (see ref 9)

3) Energy: As a check of the calculations, an energy balance was computed at selected time steps.

Kinetic Energy $T = \sum_{j=1}^{N} \sum_{k=1}^{M} \frac{1}{2} \dot{x}^2_{j,k}$

Elastic Spring Energy $V_L = \sum_{j=1}^{N} \sum_{k=1}^{M-1} \frac{1}{2} (x_{j,k+1} - x_{j,k} - 1)^2$

Shear Spring Energy $V_s = \sum_{j=1}^{N-1} \sum_{k=1}^{M} \frac{P}{2} (x_{j+1,k} - x_{j,k})^2$

Substrate Potential Energy $V_P = \sum_{j=1}^{N} \sum_{k=1}^{M} V(x_{j,k})$

where,
$$V(x) = \begin{cases} \frac{1}{2} P x^2 & |x| \leqslant \gamma \\ \frac{1}{4} P\gamma - \left[\frac{P\gamma}{1-2\gamma}\right] \left(\frac{1}{2} - |x|\right)^2 & \gamma \leqslant |x| \leqslant \frac{1}{2} \end{cases}$$

Energy lost to the surrounding medium up to time t

$$F(t) = \frac{1}{2} \sum_{j=1}^{N} \sum_{k=1}^{M} \sum_{n=1}^{NN} \dot{\eta} \dot{x}_{j,k}^2 \Delta t$$

where, NN: number of time increments

Δt: time increment

Energy lost from the boundaries up to time t

$$Q(t) = \sum_{j=1}^{N} \left(\int_0^t f_{j,M+1} \dot{x}_{j,M+1} d\tau + \int_0^t f_{j,-1} \dot{x}_{j,-1} d\tau \right)$$

where, $f_{j,M+1} = x_{j,M} - x_{j,M+1} + 1$

$f_{j,-1} = x_{j,0} - x_{j,-1} - 1$

The energy balance requires,

$T + V_L + V_S + V_P + F(t) + Q(t) = E(0)$ ⟵ initial energy

4) Logarithmic Decrement Δ_s : It is calculated by using the following method.

Let the overall dislocation velocity be

$$\dot{X}(t) = \sum_{j=1}^{N} \sum_{k=1}^{M} \dot{x}_{j,k}(t)$$

Let this function have zeroes at t_j, $j=1,2,3,\ldots$

Then, $X_j = \Delta t \sum_{n\ n_j}^{n=n_{j+1}} \dot{X}(n\Delta t)$ $\qquad n_j = \dfrac{t_j}{\Delta t}$ ← half cycle number

so that X_j approximates the area under the half cycle of the curve of $\dot{X}_j(t)$ lying between t_j and t_{j+1}. If we draw a semilog graph of X_j vs. j, 2 times the slope of the line which best fits to the points on the graph, gives the logarithmic decrement for the process [22]

VI.2 Simulation Results:

1) Energy of the system: From energy calculations, it is seen that the total energy of the system decreases steadily, while the energy lost from the boundaries increases. The sum of these two is satisfied within a few percent deviation. That deviation is at most 3%. As a result we can conclude that the results of this study are reliable.

2) Zero Peierls Stress: Figures 20 and 21 show the variation of frequency of free vibration ω_0 with $\sqrt{P}$, and period of free vibration τ_0 with dislocation loop length L.

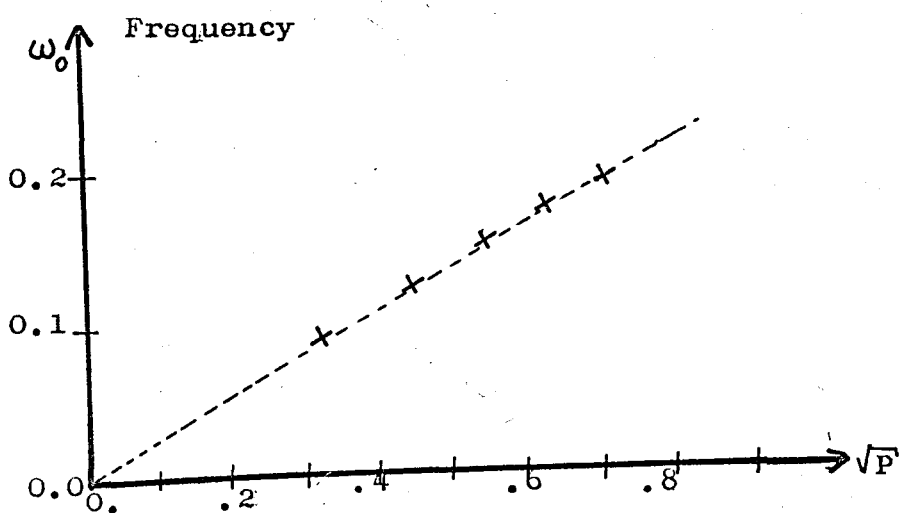

Fig. 20 Frequency ω_0 vs $\sqrt{P}$

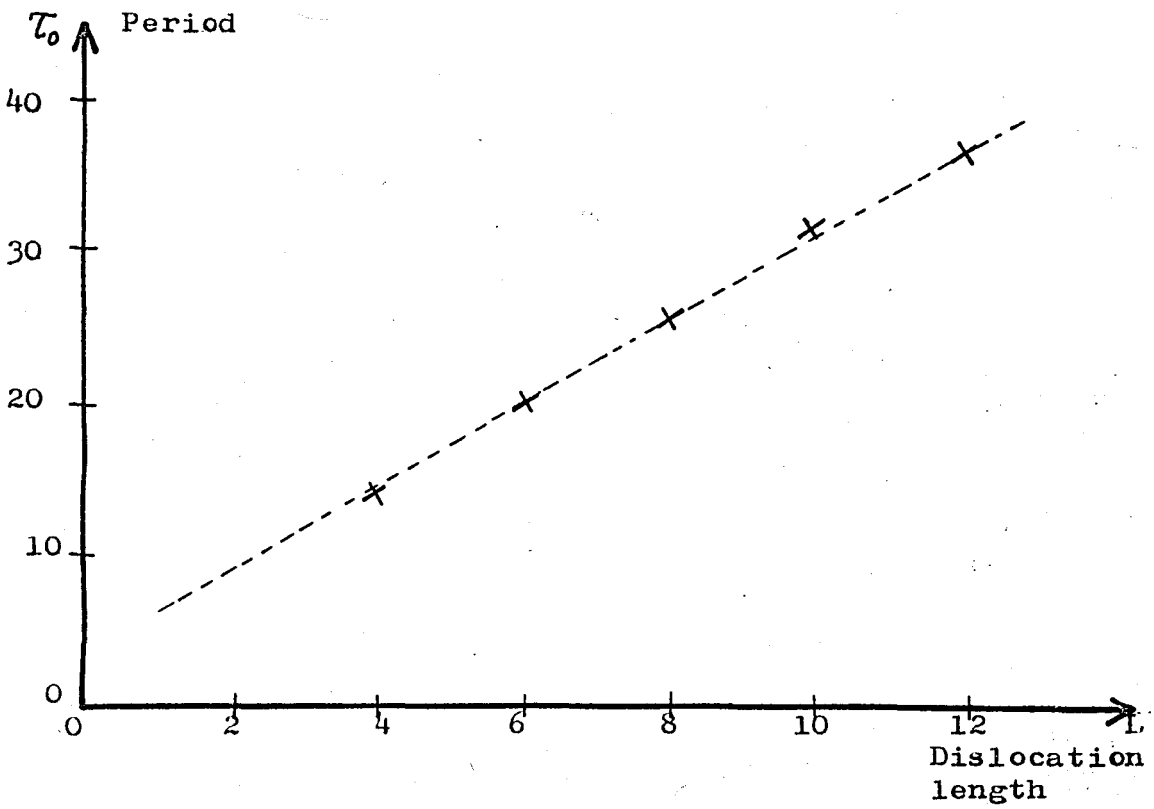

Fig. 21 Period of free vibration vs. dislocation loop length

From these two graphs, we see that the period of free vibration increases linearly with dislocation length L, and frequency increases linearly with $\sqrt{P}$, as usual.

Figures 22 and 23 show the variation of logarithmic decrement Δ_s with L and P .

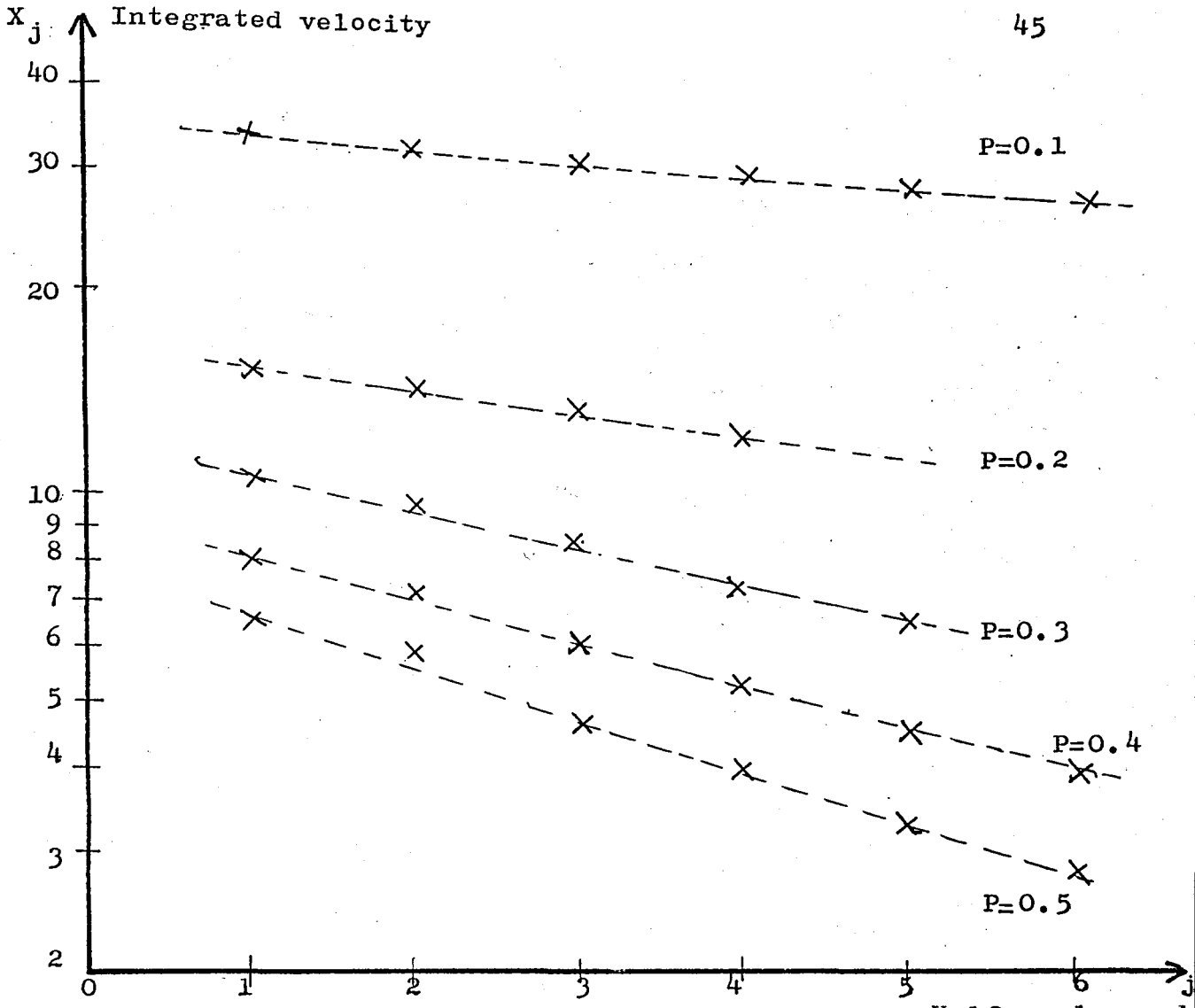

Fig. 22 Decay of X_j as a function of j for different P

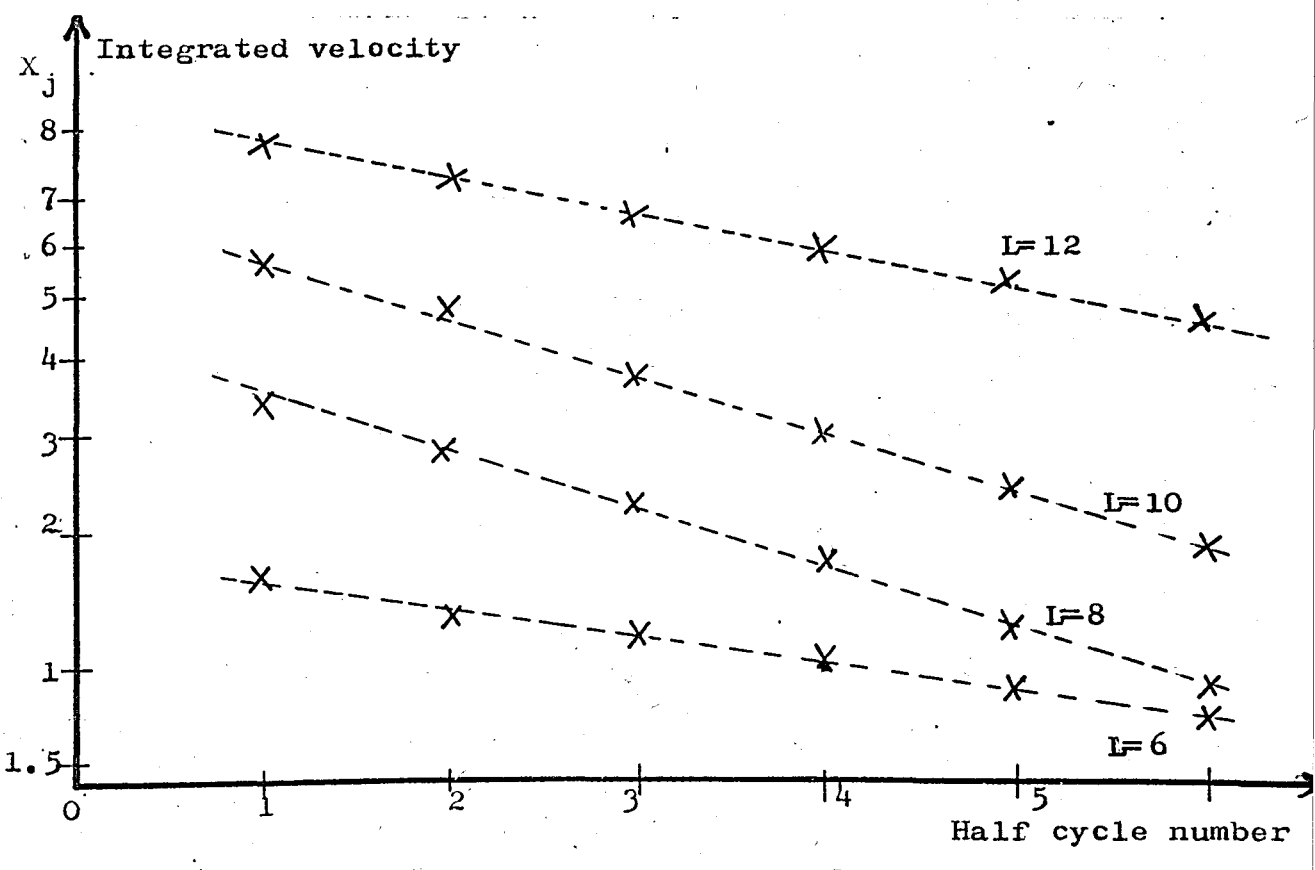

Fig. 23 Decay of X_j vs j for different L

3) Nonzero Peierls Stress: It was observed that, for any P and γ configuration, the variation of X_j with j depends on v_0 chosen. When v_0 is large enough, a linear descending curve is obtained giving the Δ_s value. But for small v_0 values, $\Delta_s=0$, showing no energy lost. This phenomena is explained by Weiner et al. [22] , as the trapping of the dislocation in a Peierls valley. For large v_0, after a certain time, $\Delta_s=0$ is reached.

Figures 24 and 25 show the change of Δ_s and τ_0 with σ_p and γ.

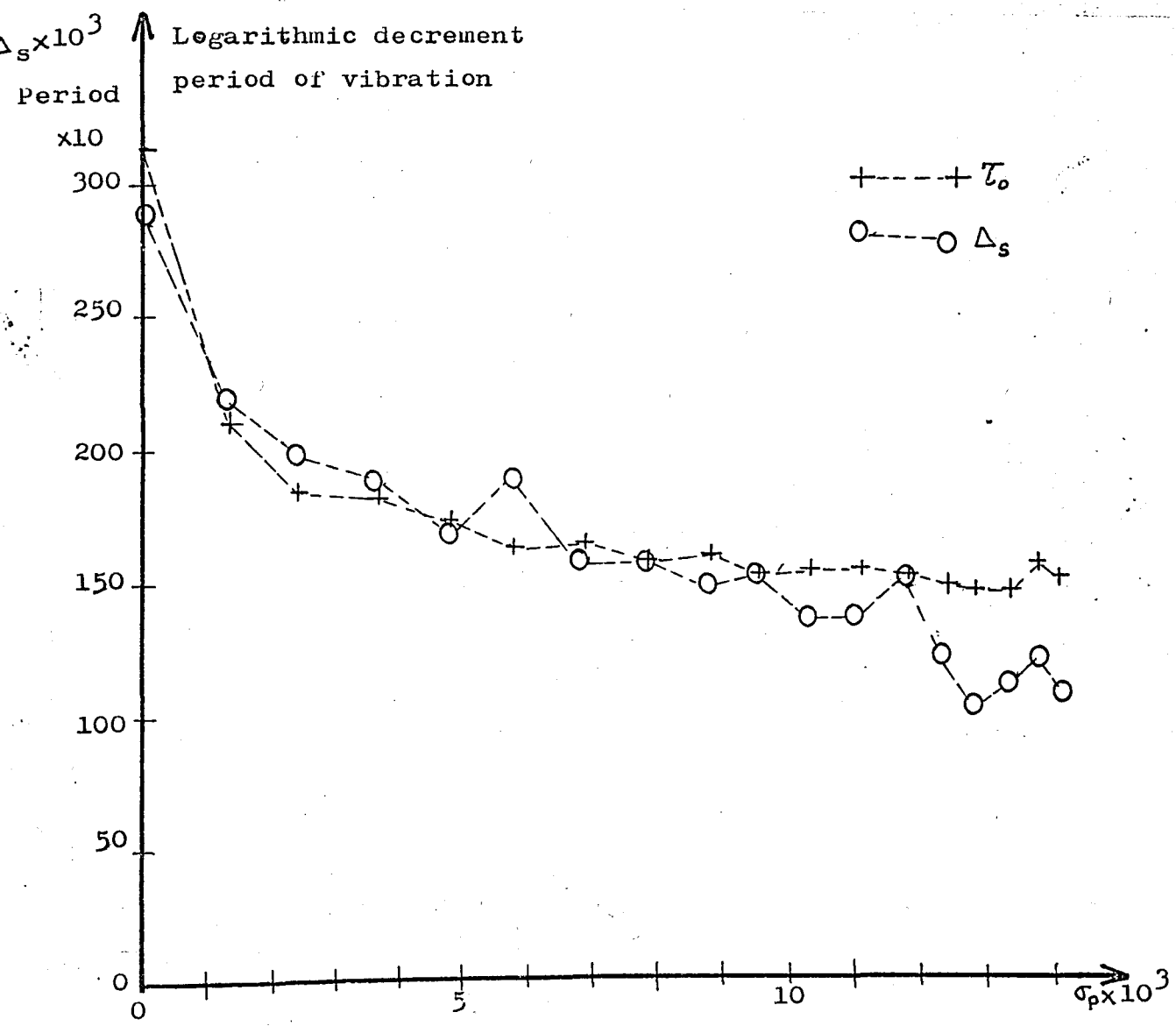

Fig. 24 Logarithmic decrement vs peierls stress
Period of vibration " " "

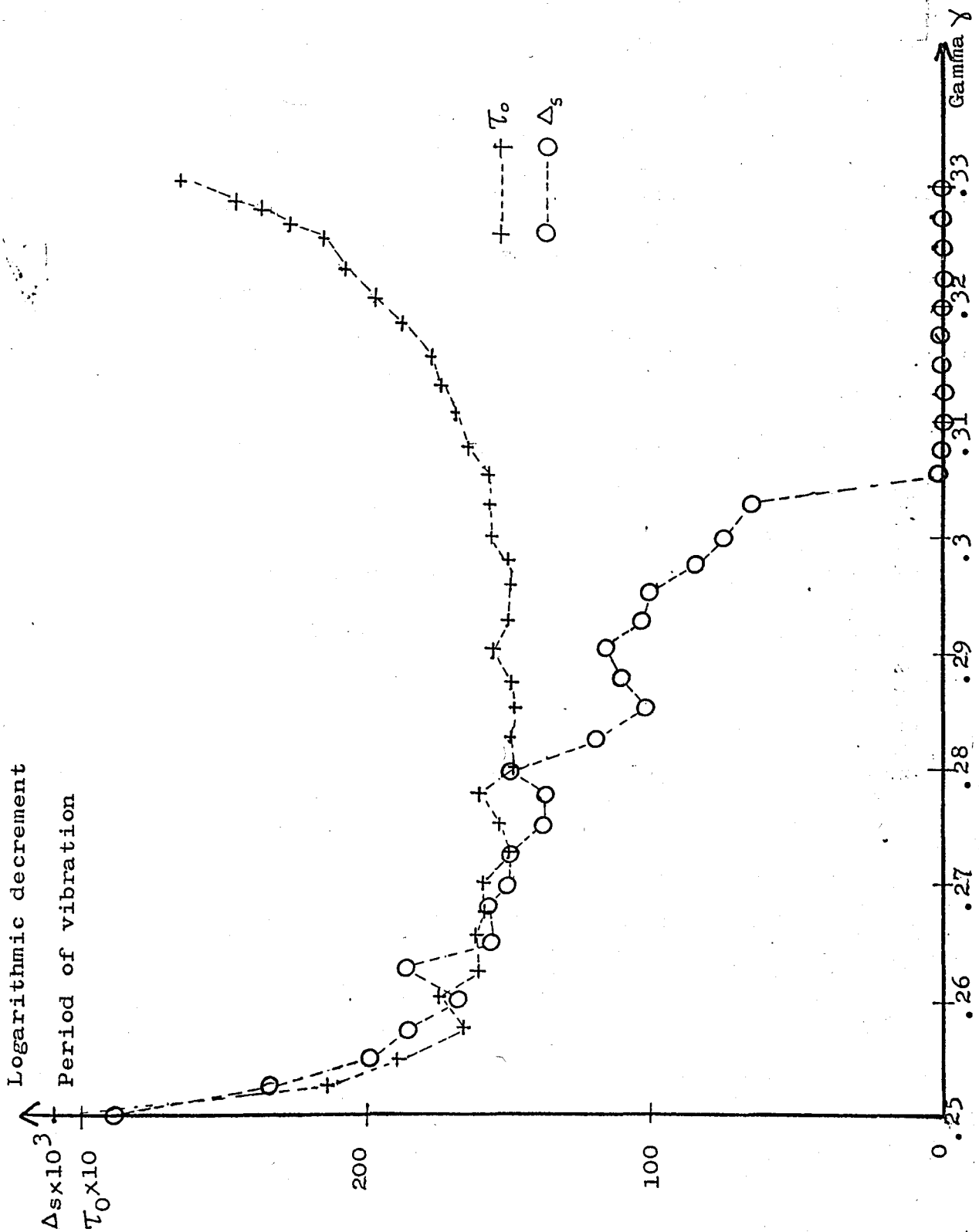

Fig. 25 Logarithmic decrement vs Gamma
Period of vibration vs Gamma

4) Effect of temperature: In order to see the effect of temperature on the dislocation vibration behaviour, random initial atomic velocities corresponding to that temperature are added to the initial velocities of the atoms. The distribution of these added velocities is a Gaussian one with zero mean and $\sqrt{\bar{v}^2}$ root mean square. The relation between T and s is $T = cs^2$

where, s : $\sqrt{\bar{v}^2}$

T : temperature in K

c : 39550 for a typical example. (NaCl) (see ref.[22])

These velocities are generated by means of a computer subroutine (RANDN) . A seed number is given as input to the subprogram, and all the atomic velocities are determined by that seed.

Fig. 26 shows the effect of temperature T on the logarithmic decrement Δ_s for three different γ values for constant P.

5) Effect of damping: When external damping is not included, the system looses energy. This energy lost is in the form of radiation. More information is given in ref. [22]. Shortly we can state that, energy loss from the vibrating dislocation may be ascribed to the imperfect transfer of energy from the localized mode associated with the dislocation in an unstable configuration U to the localized mode with the next such configuration U'. The energy which is not transferred from one localized mode

to the succeeding one is carried off by nonlocalized modes, i.e., traveling lattice waves, so that radiation energy lost occurs.

In order to see the effect of external viscous forces to the system, nonzero η values were chosen.

Fig. 27 shows X_j vs. j curve for several η values.

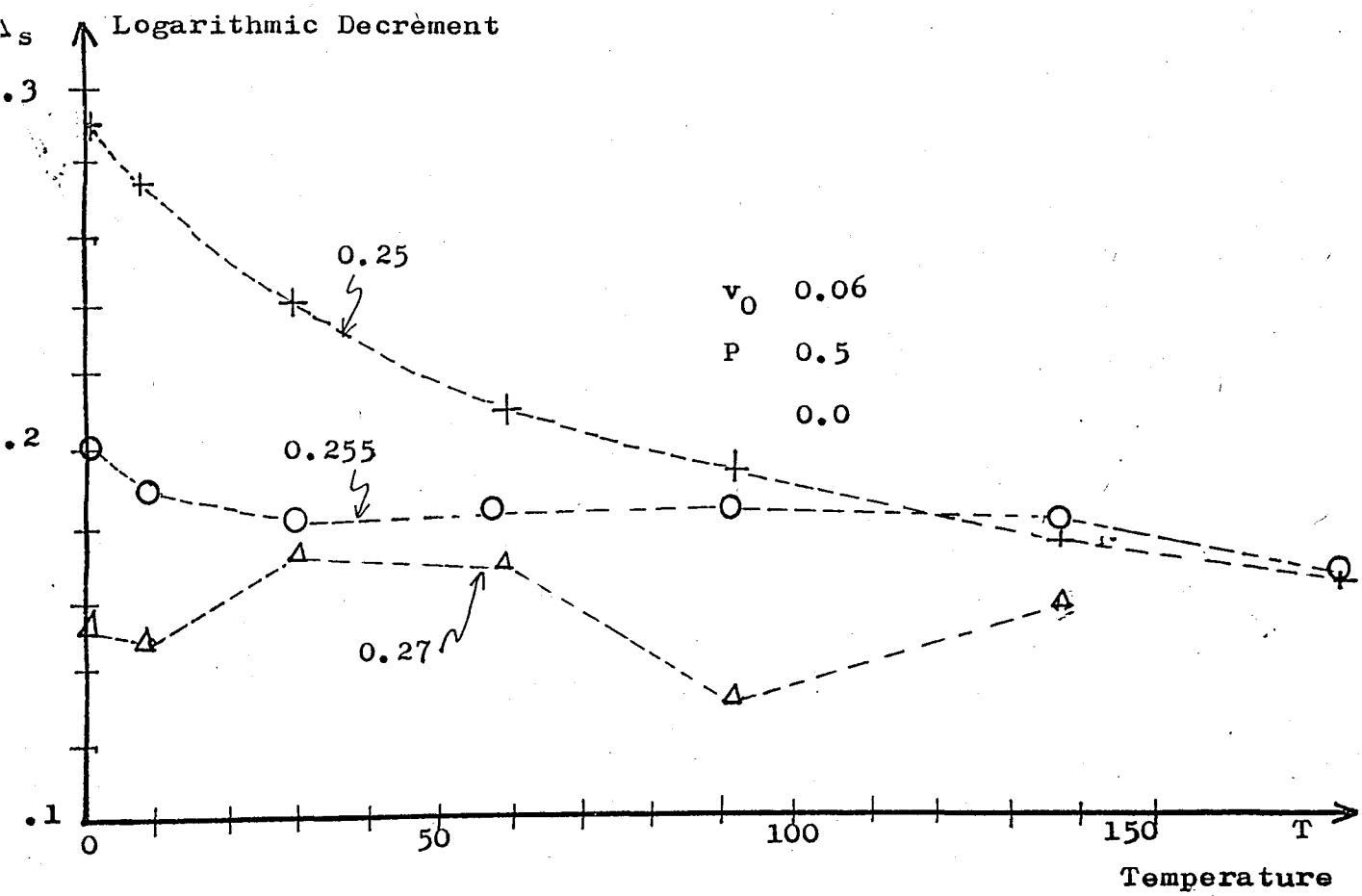

Fig. 26 Effect of temperature T on logarithmic decrement Δs for different Peierls stresses

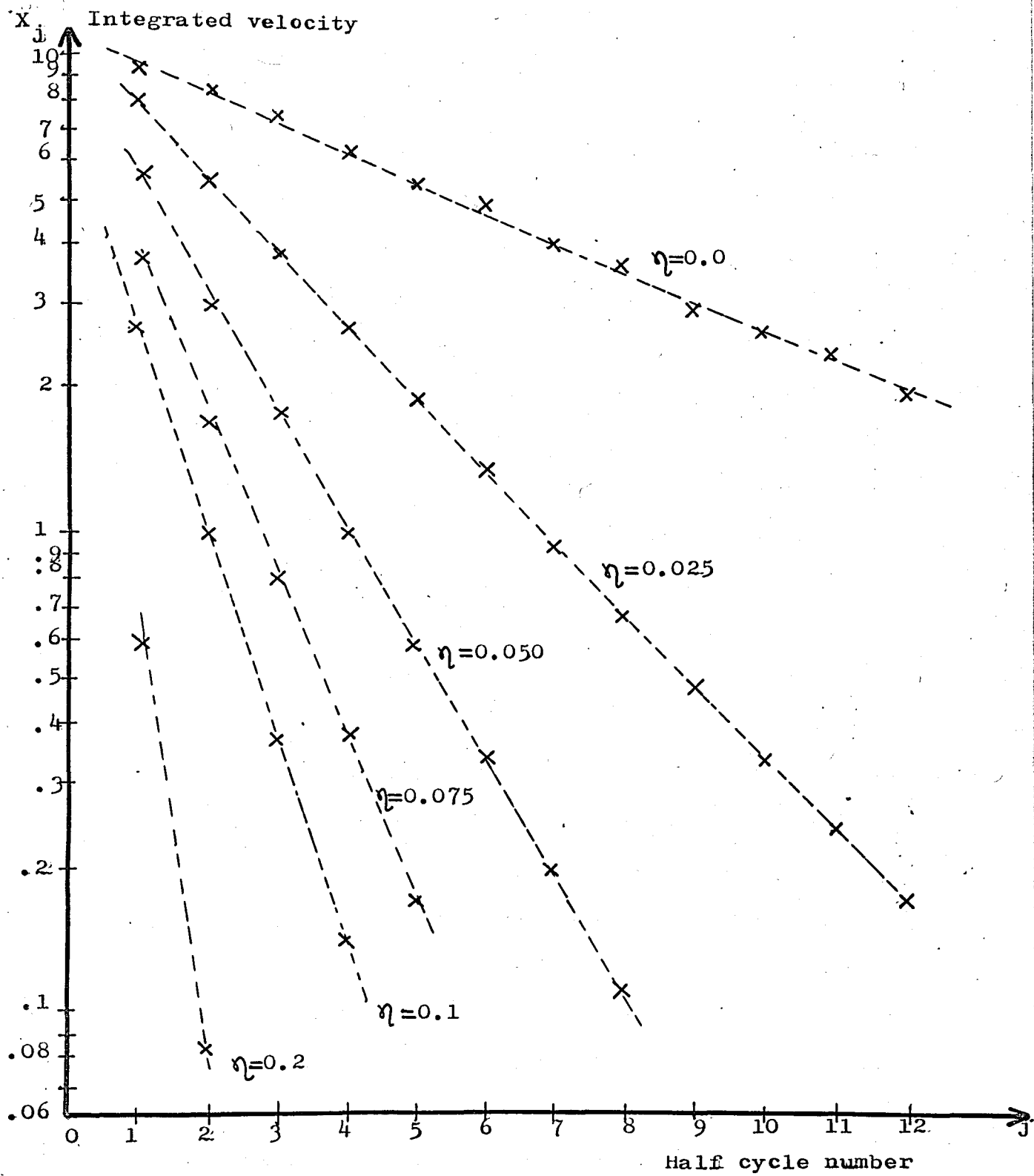

Fig. 27 Integrated velocity X_j vs half cycle number j for several η values (damping)

CHAPTER VII

DISCUSSION OF THE RESULTS

Before dealing with the simulation results, it would be better to discuss the choice of some parameters used in the simulation.

VII.1 Effect of dimensions: In the dislocation motion part, it was seen that the dislocation moves in the form of a straight line; that is, there is no interaction between rows unless the lattice has an obstruction. This observation enabled us to choose the number of rows in the lattice as small as possible. In most calculations, number of rows was three. But in order to let the dislocation to have a steady state velocity, the number of columns was chosen to be 41, in most simulations. That number proved sufficient for this purpose, at least for small stress values. By keeping column number large, the assumptions made in the model description chapter were also satisfied.

When we included an obstruction in the lattice, such as a fixed atom at the middle row, or two fixed atoms at the boundaries, row number was increased to 11, in order to let the dislocation make a bowing around the fixed atom or between the fixed atoms. It was observed that this number is not large enough, because the maximum difference between the dislocation line at the middle row

and at the end rows is around 0.5 atomic distance. It is obvious that if row number increases, this difference will increase too, and maybe the multiplication will occur. But due to computer limitations explained before, this multiplication process has not been achieved.

In the vibration part, a lattice of 20×20 (column number×row number) lattice was sufficient to satisfy the assumptions. For some parameters ($P \geqslant 0.3$) even a 10×10 lattice was enough for the purpose. For small P values ($P < 0.3$) , since the bond between rows is small, left and right boundary atoms may move larger than the permissible values, and this affects the reliability of results. To see the effect of dimensions on the energies of the system, some runs were evaluated and it was found that the difference between a 20×10 and a 30×10 lattice is very small as compared to the difference between a 10×10 and a 20×10 lattice. We can conclude that, the choice of a 20×10 lattice was a good choice; the use of larger dimensions is unnecessary.

VII.2 Effect of Δt: Most of the computations used $\Delta t = 0.209$. In order to see the effect Δt chosen, some calculations were performed by changing Δt only, while other parameters being kept unchanged, for the vibrating dislocation. The results are shown on Table 4.

parameters used:

P : 0.5 M : 20

γ : 0.25 N : 10

#	Δt	τ_0	Δ_s
1	0.419	28.274	0.334
2	0.209	28.274	0.335
3	0.140	28.274	0.346
4	0.105	28.274	0.403

Table 4 Effect of Δt

Table 4 shows that $\Delta t=0.209$ is a good choice, because the period of vibration τ_0 is constant, and logarithmic decrement Δ_s calculated do not fluctuate much by a change in Δt, around $\Delta t=0.209$. The reason for the slight change in Δ_s for very small Δt is probably due to the increased number of iterations.

VII.3 Model Parameters: Model parameter values used by Weiner et al. ([9], [10], [20]) were chosen to make a comparison. P was usually around 0.5 which is a very realistic value. Applied shear stress was within the stress range determined by the static and dynamic Peierls stresses.

In the vibration part, external damping was zero, except that the direct effect of viscosity on the calculations was observed. In dislocation motion simulations, because this external damping helps the dislocation reach its SS velocity in shorter time and distance, nonzero η values were used mostly.

Now we can discuss the results obtained, one by one:

VII.4 Dynamic Peierls stress: σ_{PD} values for two

different damping constants (η=0.1 and 0.2) are almost the same as the σ_{PD} values obtained analytically, by the use of local mode approximation. (see Fig. 5 of ref.[20])

VII.5 SS Dislocation Velocities when σ_p is present: Comparing Fig. 10 of this thesis and Fig. 6 of ref[20], we can see that the results for η=0.1 and η=0.2 cases are in good agreement. For η=0.0 case, SS dislocation velocities obtained here are less than the corresponding ones in ref. [20]. This may be a result of insufficient dimensions, because there was still a small increase in the dislocation velocity when the dislocation hits to right boundary.

The velocity stress relation will be discussed after searching the effect of Peierls stress on SS velocities.

VII.6 Effect of Peierls stress: As shown in Table 1, SS dislocation velocity does not show a clear dependance on the Peierls stress, σ_p, even though a small decrease in velocity by increasing σ_p, for small σ_p values.

VII.7 SS Dislocation Velocity when σ_p is absent: Table 3 shows that the change of P does not have a definite effect on the velocity, for a given stress, when σ_p=0. For small and large stress values, some increase is observed, but for medium stress levels, there seems to be some other factors which affect the dislocation motion.

Comparing Figures 10 and 11, we see that for a given η, the slopes of those lines are almost equal. But, the

line is cut at a stress called dynamic Peierls stress, when σ_p exists. So we can conclude that, the presence of Peierls stress does not have an important effect on velocity-stress relation, and it only produces a minimum stress level for the dislocation to be able to move.

Following the relationship given by Weertman [26]

$$\sigma b = Bv$$

where B is the damping constant, $B = A\eta$ A: a constant, so, we can derive a relation for the velocity and stress,

$$v = c\frac{\sigma}{\eta}$$

where c is a constant to be determined.

By inspecting figures 10 and 11, we see that, this relation holds for the results of this model also, with the constant c=2.5 . SS velocities found in this simulation are comparable to that of experimental methods, given in Fig. 5 of ref [26].

VII.8 USU' Motion: Counting the number of weak bond atoms at any time showed that the USU' motion assumed initially by the local mode approximation [10] is correct. For σ_p=0, UU' motion is seen (two weak bonds at any time).

VII.9 Stopping of a dislocation by an atom: In the second part of the simulation, it was observed that the presence of of a fixed atom on the path of a dislocation stops the motion of the dislocation. Due to limitations, this study couldn't be enlarged to see the multiplication of dislocations, proposed by Frank [21]. But, it is probable

that this multiplication process might be observed by increasing lattice dimensions and applying larger stresses.

The application of stress is another difficulty. Stress values used here, were in the range $\sigma_{PD} < \sigma < \sigma_P$, so we were able to apply the shear stress instantaneously, at t=0, since the stability of the model is maintained for $\sigma < \sigma_p$. Application of high stresses ($\sigma > \sigma_p$) at $t = 0$ disturbs the stability, hence, beginning with a low stress, we must increase it gradually. But, this procedure requires enormous computation time. If these problems are solved, then, it would be possible to see the multiplication of dislocations at an obstacle, and breakdown of dislocations at velocities close to the speed of sound, as explained in references [16], [18], [19] .

VII.10 Vibration of a pinned dislocation: Results given in figures 20,21,22,23 are almost the same as the results found by Weiner et al. [22] ; discussion of these figures are given in ref. [22] ; shortly we can state that, the results of a pinned dislocation are in accordance with the prediction of a string, fixed at both ends, with small damping.

Fig. 24 shows logarithmic decrement vs Peierls stress relation. Following equation 1.5 of ref. [22] ,

$$\Delta_s = \eta \tau_0$$

and observing Fig. 24 , we can state that the damping constant for the model, when a phenomenological damping is not included, is not a function of Peierls stress.

This damping is due to the energy loss from the boundaries by the traveling lattice waves.

VII.11 Temperature Effect: Fig. 26 shows that, for zero Peierls stress, the rate of decay decreases with increasing temperature. This result is not in agreement with the usual picture of the effect of temperature upon a steadily moving dislocation, an effect usually described as due to phonon drag. But the decrease in rate of decay may be due to the phenomena of " thermal energy trapping ", a process discussed by Weiner in [11] .

For nonzero Peierls stress, this decrease in rate of decay is not seen.

In fact the method used in creating thermal equilibrium at temperature T may be inaccurate. Because atoms are given an initial velocity corresponding to temperature T, only at the beginning of the computation. In a recent study, Perchak and Weiner [20] included the temperature effect in the equation of motion explicitly, and obtained more realistic results. Here, the equation of motion has a rapidly fluctuating force term $\bar{R}(\bar{t})$.

VII.12 Effect of Damping : As predicted, the rate of decay increases with external damping constant.

VII.13 Recommendations for future work: This thesis covers, mainly the stress-dislocation velocity relation, and partly the vibration characteristics of dislocations. For a continuation of this study, the following additions and modifications are possible.

1) Model: Model may be changed to simulate a more realistic crystal. A 3-D model may be used.

2) Numerical Methods: In the solution of the differential equations, some higher order approximations may be used.

3) Substrate Potential: The shape of the substrate potential may be changed to another form such that a sinusoidal one to see the differences in results of the modified and unmodified forms of Frenkel-Kontorova model.

4) Number of imperfections: By taking a very large lattice, the number of dislocations may be increased, so it would be possible to see the interaction of dislocations with each other.

5) High velocity region: By using proper stress application methods, an investigation in the high velocity region would be useful.

6) Shape of dislocation: Instead of taking a straight dislocation, a kinked dislocation may be used, so the effect of kinks on dislocation behaviour could be studied.

7) Collected Impurities: A lattice with a collection of fixed atoms could be performed in order to simulate an actual impurity.

VII.14 Closure: The most significant conclusion to be drawn from this work is that, it is possible to simulate an actual crystal with some imperfections, in the form of a computer model. Although the models in the simulation are highly idealized, they can provide valuable insight into the mechanical behaviour of materials.

REFERENCES

[1] Johnson,W.G. and Gilman,J.J., Dislocation velocities, Dislocation densities, and Plastic Flow in Lithium Fluoride Crystals, J. Appl. Phys., 30, 129 (1959)

[2] Stein,D.F. and Low,J.R., Mobility of edge dislocations in Silicon-Iron crystals, J. Appl. Phys., 31, 362 (1960)

[3] Erickson,J.S., Mobility of edge dislocations on [112] slip planes in 3.25% Silicon Iron, J. Appl. Phys., 33, 2499 (1962)

[4] Frank,F.C., on the equations of motion of crystal dislocations, Proc. Phys. Soc.,London, A62, 131 (1949)

[5] Hart,E.W., Lattice resistance to dislocation motion at high velocities, Phys. Rev., 98, 1775 (1955)

[6] Frenkel,J. and Kontorova,T., On the theory of plastic deformation and twinning, Phys. Z. Sowjetunion, 13, 1 (1938) ; 1, 137 (1939)

[7] Sanders,W.T., Peierls Stress for an Idealized Crystal Model, Phys. Rev ., 128, 1540 (1962)

[8] Kratochvil,J. and Indenbom,V.L., The Mobility of a dislocation in the Frenkel-Kontorova model, Czech. J. Phys. Rev., B13, 814 (1963)

[9] Weiner,J.H. and Sanders,W.T., Peierls Stress and Creep of a linear Chain, Phys. Rev., 134, A1007 (1964)

[10] Weiner,J.H., Dislocation Velocities in a Linear Chain, Phys. Rev., 136, A863 (1964)

[11] Weiner,J.H., Thermal Effects on Dislocation Velocities in a linear chain, Phys. Rev., 139, A442 (1965)

[12] Atkinson,W. and Cabrera,N.,Motion of a Frenkel-Kontorova Dislocation in a one dimensional crystal, Phys. Rev., 138, A763 (1965)

[13] Sanders,W.T., Dislocation Kink in a Crystal Model, J. Appl. Phys., 36, 2822 (1965)

[14] Sanders,W.T., One-Dimensional Atomic Model for a Dislocation line, Phys.Rev., 154, 654 (1967)

[15] Hartl,W.F. and Weiner, J.H., Dislocation Velocities in a Two-Dimensional Model, Phys. Rev., 152, 634 (1966)

[16] Earmme,Y.Y. and Weiner,J.H., Can dislocations be accelerated through the sonic barrier, Phys. Rev. Lett., 31, 1055 (1973)

[17] Ishioka,S., J. Phys. Soc. J., 30, 323 (1971)

[18] Earmme,Y.Y. and Weiner,J.H., Breakdown Phenomena in High-Speed dislocations, J. Appl. Phys., 45, 603 (1974)

[19] Weiner,J.H. and Pear,M.,Breakdown in high-speed edge dislocation motion, Phil. Mag., 31, 679 (1975)

[20] Perchak,D. and Weiner,J.H., Local-Mode Approximations in the Frenkel-Kontorova or sine-Gordon Chain, Phys. Rev. B, 22, 2683 (1980)

[21] Frank,F.C., On slip Bands, as a consequence of the dynamic behaviour of crystals, Report on Strength of solids, London Physical Society, 46 (1948)

[22] Weiner,J.H., Hikata, A. and Elbaum,C., Vibration of a pinned dislocation segment in an atomistic model, Phys. Rev. B, 13, 531 (1976)

[23] Weiner,J.H., Needleman,A. and Hikata,A.,Discrete String Model for Vibrating Dislocations, Internal Friction and Ultrasonic Attenuation in Solids, Univ. Tokyo Press, 503 (1977)

[24] Altıntaş,S., Dynamic Simulation of a Pinned Dislocation in an Atomistic Model, Mat. Sci. Eng., 47, 99 (1981)

[25] Rosenstock,H.B. and Newell,G.F., J. Chem. Phys., 21, 1607 (1953)

[26] Weertman,J., Dislocations in Motion, Sci. Prog., Oxf., 61, 241 (1974)

[27] Earmme,Y.Y. and Weiner,J.H., Dislocation dynamics in the modified Frenkel-Kontorova model, J. Appl. Phys., 48, 3317 (1977)

[28] Weiner,J.H. and Pear,M., Crack and dislocation propagation in an idealized crystal model, J. Appl. Phys.,46, 2398 (1975)

[29] Partom,Y., The drag force on a moving dislocation, J. Appl. Phys., 50, 4725 (1979) ; 50, 4734 (1979)

APPENDIX A DISLOCATION MOTION IN ONE DIMENSIONAL MODEL ∠

This appendix is about the choosing of proper model parameters for use in numerical computations, calculation of Peierls stress and the explanation of SUS' (stable-unstable-stable) motion of the dislocation. The model is a modification of the Frenkel-Kontorova [6] one dimensional model.

A.1 Model Description: Consider a linear chain of mass points interconnected by linear springs with spring constant k_1 and equilibrium spacing b, and subjected to a periodic potential. This substrate potential represents the effect of the remaining atoms in the 3-D crystal. Assume a piecewise quadratic, continuous potential U(x)

$$U(x)=\begin{cases}\frac{1}{2}k_2x^2 & |x|\leqslant\phi \\ \frac{1}{4}k_2\phi b - \frac{k_2\phi}{b-2\phi}\left(\frac{b}{2}-x\right)^2 & \phi\leqslant|x|\leqslant\frac{b}{2}\end{cases} \qquad (A1)$$

where,

k_2 : a measure of the shear modulus of the crystal

k_1 : " " " " Young's " " " "

ϕ : " " " " hardness " " "

In order to introduce a dislocation in this model, start with the linear chain as in Fig. A1a, and subject the j'th atom to a longitudinal force $\bar{G}_j$, where

$$\bar{G}_M=\bar{G}_{-M+1}=-\frac{1}{2}k_1b\ ;\ \bar{G}_{M-1}=\bar{G}_{-M}=\frac{1}{2}k_1b\ :,\ \bar{G}_j=0 \text{ for all other } j \qquad (A2$$

∠ This appendix is a review of the studies by Weiner and Sanders[9], Weiner[10], and Perchak and Weiner[20].

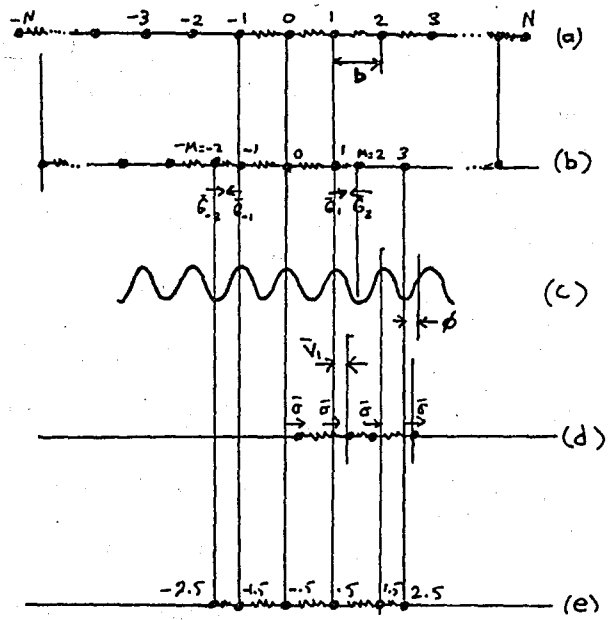

Fig A1 Linear chain dislocation model

As a result, all atoms $j \geqslant M$ are displaced b/2 to the left, all atoms $j \leqslant -M$ are displaced to the right, and those for which $-M < j < M$ are undisturbed. For the special case M=2, this new equilibrium configuration is shown in Fig. A1b . Now we have a dislocation.

Then the atoms are subjected to the substrate potential defined in equation (A1) and sketched in Fig. A1c .

Next apply forces $-\bar{G}_j$ to the configuration of A1b and A1c , annulling those originally applied, and also apply a constant force σ (external shear stress) to each atom. Let the resulting displacement of the j'th atom from the configuration of A1b be $\bar{v}_j$. With the substrate potential of equation (A1), the substrate force on the j'th atom is:

$$F_j = \begin{cases} -k_2 \bar{v}_j & \text{for } |j| \geq M, \text{ providing } |\bar{v}_j| \leq \phi \\ \dfrac{2k_2\phi}{b-2\phi}\ \bar{v}_j & \text{for } |j| < M, \text{ providing } |\bar{v}_j| \leq (\frac{b}{2} - \phi) \end{cases} \qquad (A3)$$

Note that in the first of equation (A3), $\bar{v}_j$ is measured from a potential minimum, while in the second, $\bar{v}_j$ is measured from a potential peak.

The final configuration is shown in Fig. A1d . The atoms in the range $|j| < M$ are termed subject to weak bonds to a substrate potential, while the others are referred to as strong bonds. The number of weak bonds, $n_w = 2M-1$ may be odd or even. In the latter case, the atoms are indexed as shown in Fig. A1e, that is j understood to take on the values $\ldots -1\frac{1}{2}, -\frac{1}{2}, \frac{1}{2}, 1\frac{1}{2}, \ldots$, when 2M is odd. Therefore in both cases the weak bond atoms may be taken to correspond to $-M < j < M$.

The equations of equilibrium for the configuration A1d are:

$$k_1(\bar{v}_{j+1} + \bar{v}_{j-1} - 2\bar{v}_j) - k_2\bar{v}_j - \bar{G}_j + \bar{\sigma} = 0 \quad , |j| \geq M$$
$$k_1(\bar{v}_{j+1} + \bar{v}_{j-1} - 2\bar{v}_j) + \frac{2k_2\phi}{b-2\phi}\ \bar{v}_j - \bar{G}_j + \bar{\sigma} = 0 \quad -M < j < M \qquad (A4)$$

with the introduction of dimensionless variables,

$$v_j = \bar{v}_j/b \qquad G_j = \bar{G}_j/(k_1 b) \qquad \gamma = \phi/b$$

$$\sigma = \bar{\sigma}/(k_2 b) \qquad P = k_2/k_1 \qquad Q = \frac{2\gamma P}{1-2\gamma}$$

and the reduced displacement $u_j = v_j - \sigma$

these equations may be written

$$u_{j+1} - (2+P)u_j + u_{j-1} = G_j \qquad |j| \geqslant M$$

$$u_{j+1} - (2-Q)u_j + u_{j-1} = G_j - \frac{\sigma P}{1-2\gamma} \qquad -M < j < M \qquad (A5)$$

A.2 Displacement Solution: As $N \to \infty$, the solutions are

$$u_j(\sigma; M) = (\sigma F_M + G_M)\,\beta^{-j} \quad ; \; j \leqslant -M$$

$$(\sigma F_M - G_M)\,\beta^{j} \quad ; \; j \geqslant M$$

$$u_j = \frac{\sigma(\beta - 1)\cos j\theta}{2\gamma\left(\beta\cos(M-1)\theta - \cos M\theta\right)} + \frac{(\beta-1)\sin j\theta}{2\left(\sin M\theta - \beta\sin(M-1)\theta\right)} - \frac{\sigma}{2\gamma} \; ; \quad -M < j < M \qquad (A6)$$

where, $F_M = \dfrac{\cos M\theta - \cos(M-1)\theta}{2\gamma\left(\beta^M\cos(M-1)\theta - \beta^{M-1}\cos M\theta\right)}$ $\qquad \cos\theta = 1 - \dfrac{Q}{2}$

$$G_M = \frac{\sin M\theta - \sin(M-1)\theta}{2\left(\beta^M\sin(M-1)\theta - \beta^{M-1}\sin M\theta\right)} \qquad \beta = \frac{1}{2}\left[P + 2 - (P^2+4P)^{1/2}\right]$$

A.3 Compatability and Stability of the Solution:

Assume that M, P, and σ are given. We are to determine the range of γ for which a solution with $n_w = 2M-1$ weak bonds is

i) compatible with the force law in equation (A3)

ii) mechanically stable.

i) Compatability: For compatability,

$\bar{v}_M \leqslant \phi \qquad \bar{v}_{-M} \geqslant -\phi$

$\bar{v}_{M-1} \geqslant -(b/2-\phi) \qquad \bar{v}_{-M+1} \leqslant (b/2-\phi)$

these are necessary (and sufficient).

After some manipulation , we find that

$\tan M\theta = \frac{1-\beta}{1+\beta} \operatorname{cotg} \frac{\theta}{2}$ gives lower limit on γ

(A7)

$\tan(M-1)\theta = \frac{1-\beta}{1+\beta} \operatorname{cotg} \frac{\theta}{2}$ " upper " " "

Note that γ is included implicitly in θ .

Assume that γ^{-1} which satisfies the first equation is denoted by C_M , and the second equation by C_{M-1}

then, $C_{M-1} \leqslant \gamma^{-1} \leqslant C_M$

(the lowest value of θ must be chosen not to violate the inequalities of (A3) except the ones for $j=M$)

ii) Stability: After the necessary calculations, it is found that, the solution corresponding to 2M-1 weak bonds will be stable only for

$\gamma^{-1} \geqslant C_{M-\frac{1}{2}}$ where, $C_{M-\frac{1}{2}}$ is given by

$\tan(M-\frac{1}{2})\theta = \frac{1-\beta}{1+\beta} \operatorname{cotg} \frac{\theta}{2}$ upper limit for stability

Combining stability and compatability results,

$C_{M-\frac{1}{2}} \leqslant \gamma^{-1} \leqslant C_M$

If the value of γ^{-1} is in the range given above, a solution with 2M-1 weak bonds is both compatible and

stable, while the only other compatible solution for the same γ , that with one more weak bond is unstable.

A.4 γ Ranges for M=1 and M=3/2 :

1) M=1

$$\tan\theta = \frac{1-\beta}{1+\beta}\ \cot g\frac{\theta}{2} \longrightarrow \gamma = 0.25$$

$$0 = \frac{1-\beta}{1+\beta}\ \cot g\frac{\theta}{2} \longrightarrow \gamma = 0.4444$$

$$\tan\frac{1}{2}\theta = \frac{1-\beta}{1+\beta}\ \cot g\frac{\theta}{2} \longrightarrow \gamma = 0.3333$$

2) M = 3/2

$$\tan\frac{3}{2}\theta = \frac{1-\beta}{1+\beta}\ \cot g\frac{\theta}{2} \longrightarrow \gamma = 0.1928$$

$$\tan\frac{1}{2}\theta = \frac{1-\beta}{1+\beta}\ \cot g\frac{\theta}{2} \longrightarrow \gamma = 0.3333$$

$$\tan\theta = \frac{1-\beta}{1+\beta}\ \cot g\frac{\theta}{2} \longrightarrow \gamma = 0.25$$

If we draw γ axis,

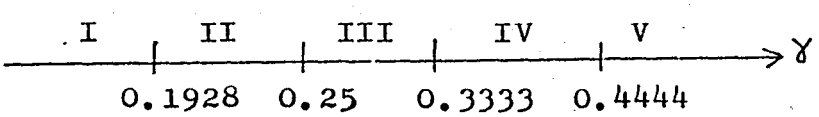

Regions I and V: The solution is not compatible and stable for M=1, or M=3/2

Region II :The solution is compatible and stable for M=3/2; not compatible and not stable for M=1

Region III: The solution is compatible and stable for M=1; compatible but not stable for M=3/2

Region IV: The solution is not compatible and not stable for M=3/2; compatible but not stable for M=1.

These values are calculated for P=0.5

A.5 Peierls Stress:

Equations of stability show that

$$\sigma \leqslant \frac{\gamma + \beta^{M} G_M}{1 + \beta^{M} F_M} \qquad \sigma \leqslant \frac{\gamma + \beta^{M-1} G_M}{1 + \beta^{M-1} F_M}$$

σ_p is defined as the stress above which these inequalities are invalid.

Of these two, the first one is the controlling.

By substituting the variables,

$$\sigma_p = \gamma \left[\frac{\cos M\theta - \beta \cos(M-1)\theta}{\sin M\theta - \beta \sin(M-1)\theta} \right] \times \left[\frac{\sin M\theta - \delta \sin(M-1)\theta}{\cos M\theta - \delta \cos(M-1)\theta} \right]$$

where $\delta = \beta(2\gamma-1)/(2\gamma-\beta)$

A.6 Change of σ_p with γ, for different P values:

Fig. A2 shows the variation of σ_p with γ, for M=1 and M=3/2, and for different P values. (P=0.3, 0.5, 0.7)

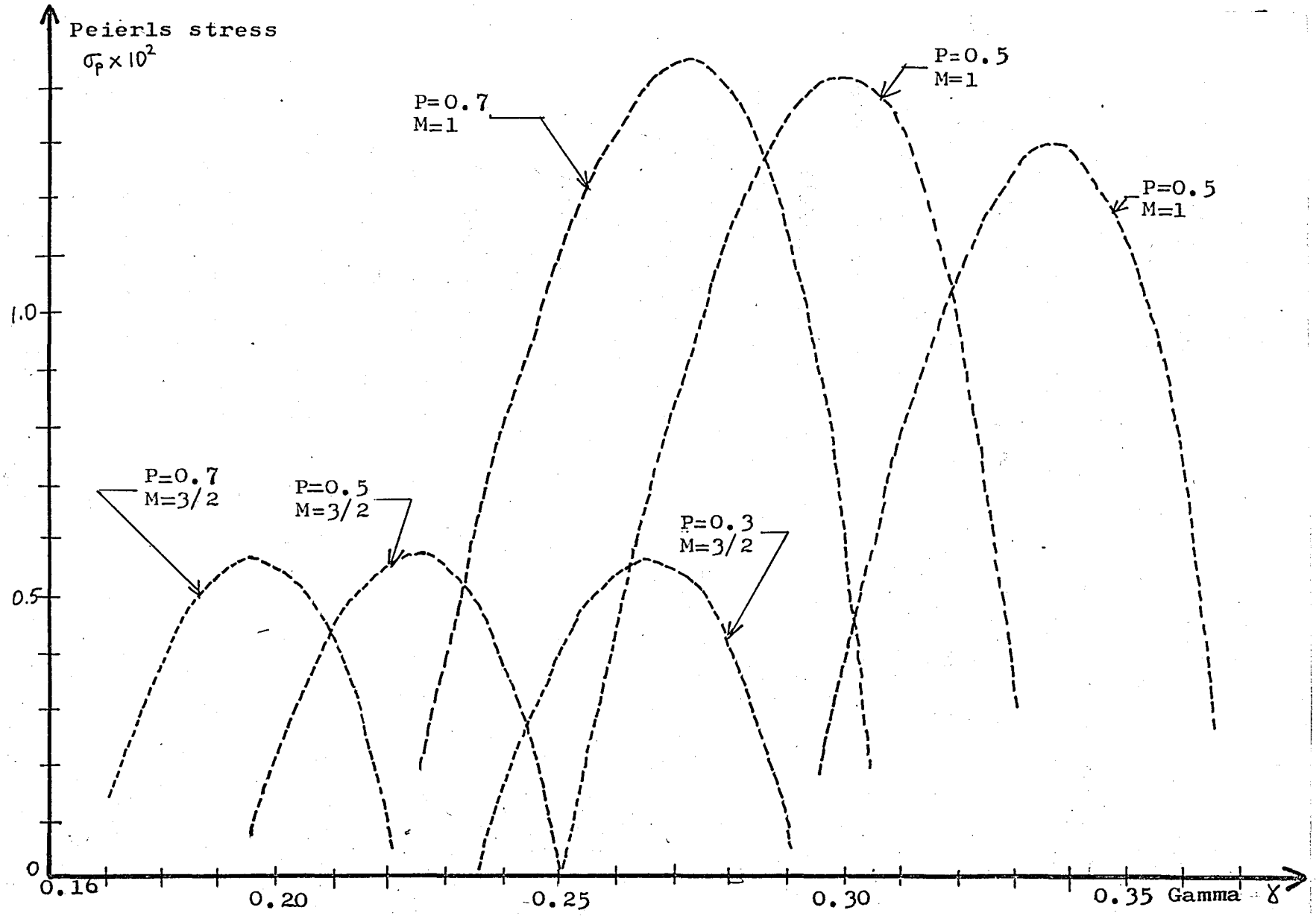

Fig. A2 Peierls stress σ_p vs gamma γ for different parameter values of P and M

A.7 Dynamic Peierls Stress: It was shown that the Peierls stress σ_P is the stress required under quasi-static conditions and in the absence of thermal motion to move the dislocation from one stable equilibrium position to an adjacent one. However, once the dislocation is in motion, i. e. , has surpassed one potential barrier, it acquires kinetic energy and continued motion will be possible at lower stress values. This stress is called the Dynamic Peierls Stress σ_{PD}.

A.8 Stable and Unstable Positions: We have seen before that for a given set of P and γ , there exist two equilibrium configurations for the dislocation:

1) Stable configuration with $n_w = 2M-1$ weak bonds,

2) Unstable configuration with one more weak bond.

For example, let P=0.5 and γ=0.3

if M=1 the configuration is stable, and

if M=3/2 the configuration is unstable.

This situation holds as long as the applied stress σ is less than σ_P (Peierls stress) .

For $\sigma \geq \sigma_P$ no stable equilibrium solution exists.

A.9 Motion of the dislocation: Let the dislocation be in the successive configuration as in Fig. A3.

This motion can be described as the motion of a series of alternately suspended (stable) and inverted (unstable) pendulums. (Fig. A4)

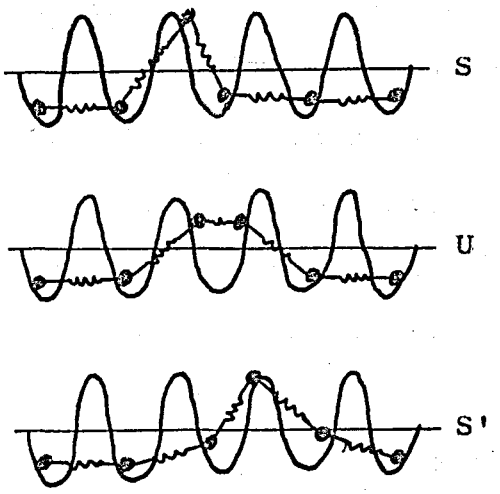

Fig. A3 Sequence of atom states

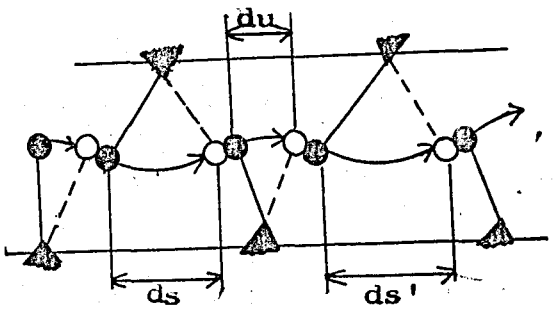

Fig. A4 Pendulum analogy

In ref. [10], it is given that the energy transfer at transition times from S to U or from U to S, energy transfer is partial.

Another analogy is the movement of a ball on a mountain chain with certain obstructions, which absorbs part of the energy of the ball. (Fig. A5)

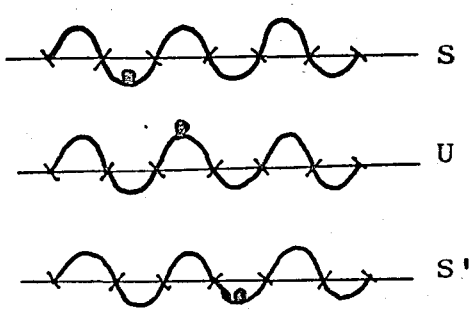

Fig. A5 Ball analogy

It is clear that, during motion, if the ball comes to the top of a hill (unstable equilibrium point), then, it will be able to reach the top of second hill by the help of dynamic Peierls stress, σ_{PD} . But if it is stationary in a well, then, the necessary stress to take it to the top of a hill is the Peierls stress, σ_{P} . After it reaches the top, it will continue to move.

After this discussion, we can state that the motion of the dislocation model depends on the initial conditions. If atoms are in stable equilibrium positions (M=1), at least Peierls stress is necessary to move the dislocation, but if they are in unstable equilibrium positions (M=3/2), dynamic Peierls stress is sufficient to move it. As a result, it is possible to calculate the Peierls stress (or dynamic Peierls stress) for a given set of parameters, experimentally (by computer simulation) by only choosing the stable (or unstable) equilibrium configuration for the atoms by the use of proper formulae given in part A.2 , applying any stress σ , and observing if the dislocation moves. The minimum stress which will make the dislocation move is the Peierls stress (or the dynamic Peierls stress).

Addition of damping and temperature brings some complexity to this discussion; these topics are studied by Perchak and Weiner [20] in detail. In that paper, [20] , steady state velocities of the dislocation under certain parameters are calculated by computer simulation and

analytically. Good agreement is found between the results of these calculations.

In this thesis, a two dimensional model is used. Initial configuration is such that the atoms in any row are in unstable equilibrium positions for zero applied stress; there is no difference between rows. Then, a stress $\sigma_{PD} \leqslant \sigma \leqslant \sigma_{P}$ is applied and steady state velocity of the dislocation is calculated. The results are compared to that of the one-dimensional results of the studies explained in this appendix.

APPENDIX B PHYSICAL INTERPRETATIONS OF THE PARAMETERS USED IN COMPUTER SIMULATION

In the computer simulation of dislocation model, dimensionless quantities were used to simplify the calculations, and to generalize the model. This appendix explains the meanings of the dimensionless variables, and gives numerical information in CGS units, about the true values of these parameters.

A typical example is NaCl crystal with the following properties:

Density : 2.17 gm/cm^3

Shear Modulus G : 1.26×10^{11} dyn/cm^2

Young's Modulus E : 5.0×10^{11} dyn/cm^2

Lattice Constant b : 2.8×10^{-8} cm

B.1 position or distance: It is defined as $\bar{x}/b$, where $\bar{x}$ is the true length. To find the actual distance, the nondimensional distance x must be multiplied by lattice constant b.

for example, 1 atomic distance means $\bar{x}= 2.8\times10^{-8}$ cm.

B.2 linear spring constant k_1: It is a measure of Young's Modulus E. Assuming the proportionality constant to be b,

$$k_1= E\times b =5.\times10^{11} \text{ dyn/cm}^2\times 2.8\times10^{-8} \text{ cm}$$

$$k_1= 1.4\times10^{4} \text{ dyn/cm}$$

B.3 shear spring constant k_2: It is a measure of shear modulus G. Assuming the proportionality constant to be b,

$$k_2 = G \times b = 1.26 \times 10^{11} \text{ dyn/cm}^2 \times 2.8 \times 10^{-8} \text{ cm}$$

$$k_2 = 1.4 \times 10^{4} \text{ dyn/cm}$$

B.4 Ratio of shear spring constant to linear spring constant, P:

$$P = k_2/k_1 = G/E$$

usual range for P : 0.2 - 0.5

B.5 time t :

$$\bar{t} = t\sqrt{\frac{m}{k_1}} \qquad m = \rho b^3, \quad k_1 = bE$$

$$\bar{t} = t\sqrt{\frac{\rho b^3}{bE}} = tb\sqrt{\frac{\rho}{E}}$$

$$\bar{t} = t \times 2.8 \times 10^{-8} \text{ cm} \times \sqrt{\frac{2.17 \text{ gm/cm}^3}{5. \times 10^{11} \text{ dyn/cm}^2}}$$

$$\bar{t} = t \times 5.833 \times 10^{-14} \text{ sec}$$

every dimensionless time is around the order of 10^{-14} sec.

B.6 velocity v:

$$\bar{v}=\frac{\bar{x}}{\bar{t}}=\frac{bx}{t}\times\sqrt{\frac{k_1}{m}}=\frac{bx}{t}\sqrt{\frac{k_2}{m}}\frac{1}{\sqrt{P}}=\frac{x}{t}\sqrt{\frac{Gb^3}{\rho b^3}}\frac{1}{\sqrt{P}}$$

$$\bar{v}=\frac{x}{t}\times\sqrt{\frac{\mu}{\rho}}\times\frac{1}{\sqrt{P}}=\frac{x}{t}c_S\frac{1}{\sqrt{P}} \quad \text{where } c_S=\sqrt{\frac{\mu}{\rho}}=c_L\sqrt{P}$$

c_S: transverse wave speed

c_L: longitudinal " "

$$\bar{v}=c_L\frac{x}{t} \qquad \bar{v}=c_L v$$

unit dimensionless velocity represent the velocity of longitudinal waves in crystal when the substrate potential is neglected.

For NaCl , $c_S=\sqrt{\frac{\mu}{\rho}}=\sqrt{\frac{G}{\rho}}=2.4\times10^5$ cm/s

$$c_L=\frac{c_S}{\sqrt{P}}=\frac{2.4\times10^5}{\sqrt{\frac{1.26\times10^5}{5.\times10^5}}}=4.8\times10^5 \text{ cm/s}$$

$v=1$ means speed of sound. (4.8×10^5 cm/s for NaCl)

B.7 Stress σ :

$\bar{\sigma}=\sigma k_2 b$ ← definition

$\bar{\sigma}=\sigma Gbb=\sigma Gb^2$

$\bar{\sigma}=\sigma\times1.26\times10^{11}$ dyn/cm$^2\times(2.8\times10^{-8})^2$ cm^2

$\bar{\sigma}=9.88\times10^{-5}$ dyn ← force

or, $\bar{\sigma}_s=\bar{\sigma}/b^2=1.26\times10^{11}$ dyn/cm^2 ← stress

For example, $\sigma=1.42\times10^{-2}$ means

$\bar{\sigma}=1.8\times10^9$ dyn/cm^2 , or

$\bar{\sigma}_s=1.4\times10^{-6}$ dyn/ unit atomic area

ACKNOWLEDGEMENTS

I would like to express my gratitude to my thesis supervisor, Dr. Sabri Altıntaş for his helpful discussions without which this thesis would not have been possible. I also appreciate his guidance and encouragement.

Thanks are also due to Doç.Dr. Öktem Vardar and Doç.Dr. Başar Civelek for their interest, encouragement and help during this study.